Diazabicyclooctane Functionalization for Inhibition of β-Lactamases from Enterobacteria

Flavie Bouchet, Heiner Atze, Matthieu Fonvielle, Zainab Edoo, Michel Arthur, Mélanie Etheve-Quelquejeu, Laura Iannazzo

DIAZABICYCLOOCTANE FUNCTIONALIZATION FOR INHIBITION OF β-LACTAMASES FROM ENTEROBACTERIA

Flavie Bouchet,[†1] Heiner Atze,[‡1] Matthieu Fonvielle,[‡] Zainab Edoo,[‡] Michel Arthur,[‡*] Mélanie Ethève-Quelquejeu,[†*] Laura Iannazzo[†*]

[†]Laboratoire de Chimie et de Biochimie Pharmacologiques et Toxicologiques, Université de Paris, UMR 8601, Paris, F-75006 France ; CNRS UMR 8601, Paris, F-75006, France.

[‡] INSERM, Sorbonne Université, Université de Paris, Centre de Recherche des Cordeliers, F-75006, Paris, France.

ABSTRACT: Second-generation β-lactamase inhibitors containing a diazabicyclooctane (DBO) scaffold restore the activity of β-lactams against pathogenic bacteria, including those producing class A, C, and D enzymes that are not susceptible to first-generation inhibitors containing a β-lactam ring. Here, we report optimization of a synthetic route to access triazole-containing DBOs and biological evaluation of a series of 17 compounds for inhibition of five β-lactamases representative of enzymes found in pathogenic Gram-negative bacteria. A strong correlation (Spearman coefficient of 0.87; p = 4.7 10^{-21}) was observed between the inhibition efficacy of purified β-lactamases and the potentiation of β-lactam antibacterial activity indicating that DBO functionalization did not impair penetration. In comparison to reference DBOs, avibactam and relebactam, our compounds displayed reduced efficacy due to the absence of hydrogen bonding with a conserved asparagine residue at position 132. This was partially compensated by additional interactions involving certain triazole substituents.

Penicillin is the first antibiotic introduced in medicine and the β-lactams remain the most widely used drug family in spite of the emergence of various resistance mechanisms.[1] The targets of β-lactams are the D,D-transpeptidases, commonly referred to as penicillin-binding proteins (PBPs), that catalyze the last cross-linking step of peptidoglycan synthesis.[2] The most common β-lactam resistance mechanism in Gram-negative bacteria is the production of one or more β-lactamases, which catalyze the hydrolysis of the amide bond of the four-membered β-lactam ring (Figure 1A).[3] The hydrolysis product is not active accounting for the absence of inhibition of the PBP targets. This resistance mechanism has been successfully defeated by β-lactamase inhibitors, clavulanate, sulbactam, and tazobactam (Figure 1B).[3, 4] In the presence of these inhibitors, the drug (imipenem in Figure 1C) remains active for acylation of the PBPs. First-generation inhibitors contain a β-lactam ring and act as suicide substrates forming stable adducts with β-lactamases (Figure 1C).[3] Avibactam (Figure 1B), clinically approved in combination with ceftazidime in 2015, is the first representative of second-generation inhibitors. Its structure is based on a distinct scaffold, diazabicyclooctane (DBO), which contains a five-membered cyclic urea rather than a β-lactam ring.[5, 6] The mechanism of action of avibactam relies on nucleophilic attack of the DBO carbonyl by the active serine of the β-lactamase leading to regioselective opening of the cyclic urea and nitrogen protonation (Figure 1D).[6] This reaction affords a stable carbamoyl-enzyme adduct. In contrast to β-lactam-containing inhibitors, formation of the carbamoyl-enzyme is fully reversible regenerating native β-lactamase and avibactam.[6-8] The efficacy of avibactam relies on the stabilization of the adduct that displaces the equilibrium toward the covalent carbamoyl-enzyme. Stabilization is also important to prevent carbamoyl-enzyme hydrolysis, which proceeds through an initial desulfonation for certain β-lactamases.[9-11] Compared to the first- generation inhibitors, avibactam inhibits a wider range of β-lactamases (class A, C, and some class D enzymes).[3] In particular, avibactam inhibits β-lactamases that are fully insensitive to inhibition by clavulanate, such as *Klebsiella pneumoniae* carbapenemases (KPC) and *Mycobacterium abscessus* Bla_{Mab}.

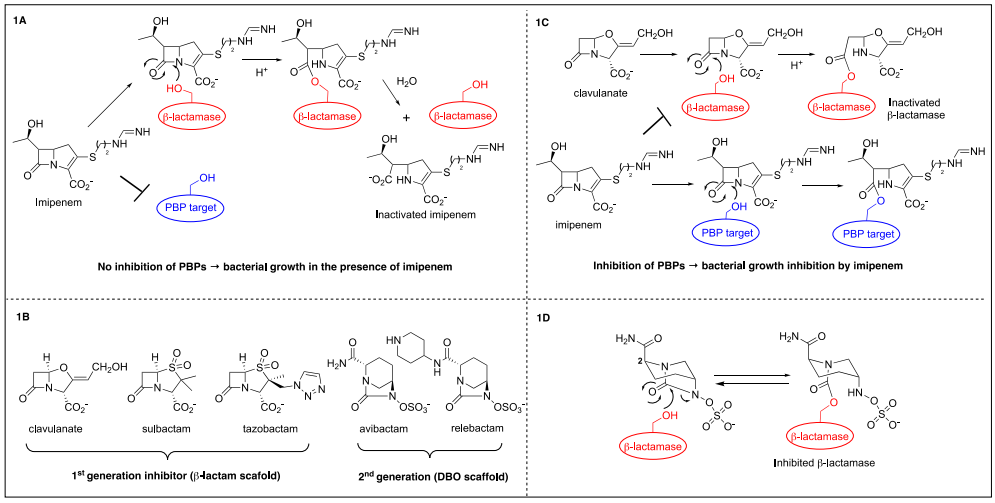

Figure 1. Structure and mode of action of antibiotics and β-lactamase inhibitors. (1A) β-lactamase-mediated resistance to imipenem. (1B) Structure of 1st and 2nd generation β-lactamase inhibitors based on β-lactam and diazabicyclooctane (DBO) scaffolds, respectively. (1C) Mode of action of a β-lactamase inhibitor (clavulanate), which prevents imipenem hydrolysis enabling inactivation of the penicillin-binding protein (PBP) targets. (1D) Avibactam-mediated β-lactamase inhibition by reversi-

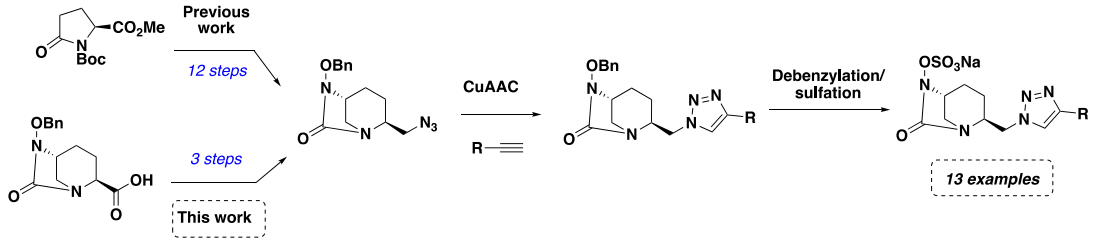

Scheme 1. Strategies to access functionalized DBOs.

Functionalization of the DBO scaffold has been extensively explored to improve their β-lactamase inhibition spectra.[12-20] In addition, introduction of side chains was reported to afford dual inhibitors that act both on β-lactamases and on essential penicillin-binding proteins required for cell wall peptidoglycan polymerization.[12] Since DBOs are chemically challenging molecules in terms of their structures, we recently developed a versatile method using copper-catalyzed alkyne-azide cycloaddition (CuAAC) to introduce 1,2,3-triazole-containing substituents at the C_2 position of the DBO scaffold.[21] Here, we report optimization of our synthetic scheme, including the sulfation step (Scheme 1), which enabled synthesis of a series of compounds in sufficient amount for biological evaluation of a panel of five representatives of class A, C, and D β-lactamases. This evaluation involved both the determination of kinetic parameters for β-lactamase inhibition and evaluation of antibacterial activity against isogenic strains producing specific β-lactamases.

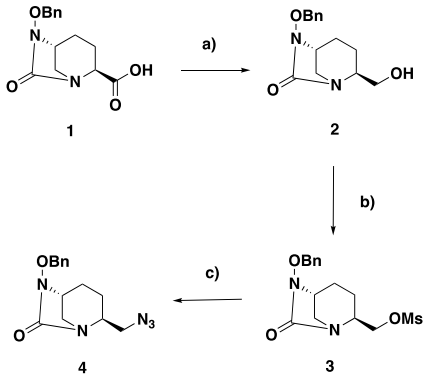

Scheme 2: a) i. $ClCO_2iBu$, NEt_3, THF, 0°C, 2h, ii. $NaBH_4$, 0°C, 3h; b) MsCl, DMAP, NEt_3, DCM, 0°C, 2h; 3) NaN_3, DMF, 90°C, 20h *(35% over 3 steps)*.

Chemical synthesis. We recently reported the synthesis of 2-azido-diazabicyclooctane **4** starting from commercially available protected oxopyrrolidine (Scheme 1).[21] This 12-step procedure provided access to the key intermediate for the copper(I)-catalyzed Huisgen-Sharpless cycloaddition reaction[22] with an overall yield of 4%. Here, we propose a shorter and more efficient approach starting with the carboxylic acid DBO derivative **1**, which has recently been made commercially available. DBO **1** was activated with *iso*-butylchloroformate and directly reduced with $NaBH_4$ to afford the corresponding alcohol **2** (Scheme 2). Activation of **2** with mesylchloride followed by a nucleophilic substitution in the presence of sodium azide provided azido derivative **4**. Using this strategy,

the azido-DBO **4** was synthesized in 35% yield over 3 steps without purification of the alcohol and the mesylated intermediates. The functionalization of **4** was then explored with various alkynes to afford a series of new DBOs (Table 1). Briefly, alkynes **5a**, **5b**, **5c**, **5d**, **5e**, **5h**, and **5j** were commercially available whereas **5f**, **5g**, and **5i** were prepared according to standard procedures (See supporting information). Compound **4** and alkynes **5a-j** were subjected to CuAAC conditions using $CuSO_4$ (30 mol %) and sodium ascorbate (60 mol %) in THF/H_2O overnight at room temperature to afford compounds **6a-j** in 30 to 97% yield (Scheme 3). A wide range of alkynes was compatible with this procedure including compounds containing aromatic rings, such as pyridine (**5a**) and phenyl (**5b, 5i**), Si, O, or N heteroatoms (**5c-f**), a protected amine (**5g-i**), or a carboxylic acid function (**5j**). The deprotection of the benzyl group of compounds **6a-j** was performed by hydrogenolysis followed by sulfation with sulfur trioxide pyridine complex. The purification of the final compounds **7a-j** has been optimized by elution through DOWEX Na^+ followed by the dissolution of the residue in ethanol and filtration. This additional step was helpful for an efficient purification of DBOs over HPLC and allowed increasing the overall sulfation yield (from 10% for compounds **7a** and **7c** according to the previous method[21] to 21% and 14%, respectively, in the current study). The final deprotection step for Boc-containing DBOs (**7g**, **7h**, and **7i**) was performed by treatment with TFA in DCM at 0°C for 1 h (Scheme 4). Unprotected DBOs **8g**, **8h**, and **8i** were isolated in 36, 34 and 17% yield after HPLC purification, respectively. To get access to unsubstituted triazoles **10a** and **10b** (Scheme 5), a new strategy has been designed. The alcohol **2** was activated with mesylchloride and treated with 1H-1,2,3-triazole under basic conditions[23] to afford regioisomers **9a** and **9b** in 44 and 37% yield, respectively. After separation of the two regioisomers by chromatography, each compound was submitted to hydrogenolysis conditions to remove the benzyl group followed by the sulfation step and elution on DOWEX Na^+, as described above.

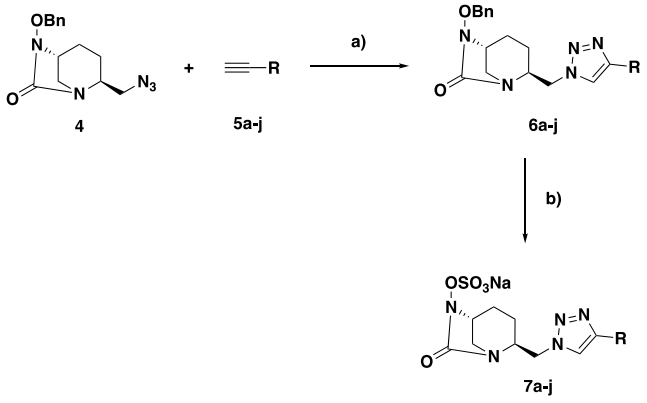

Scheme 3. a) $CuSO_4$ 30 mol %, sodium ascorbate 60 mol %, THF/H_2O (3/1), rt, overnight; b) i. Pd/C, H_2, MeOH, rt, 48 h, ii. SO_3-Pyr, pyridine, rt, overnight, iii. DOWEX Na^+.

Rationale for *in vivo* evaluation of DBOs. We chose a panel of five β-lactamases that are clinically relevant, belong to different structural classes, and differ by their hydrolysis spectrum.[3] KPC-2 (class A) and OXA-48 (class D) hydrolyze carbapenems (carbapenemases), which are often the last resort antibiotics against multi-drug-resistant bacteria. CTX-M-15 and AmpC from *Enterobacter cloacae* were chosen as representatives of class A extended-spectrum β-lactamases and of class C cephalosporinases (preferential hydrolysis of cephems). TEM-1 is a wide-spread representative of penicillinases (preferential hydrolysis of penams). Genes encoding these five β-lactamases were cloned under the control of an inducible promoter into the vector pTR99k and introduced in *Escherichia coli* Top10. The efficacy of the DBOs was tested by determining the minimal inhibitory concentration (MIC) of β-lactams in the presence or absence of a fixed concentration of inhibitor (15 μM corresponding to 4 μg/ml for avibactam). Since the TEM-1, KPC-2, CTX-M-15, AmpC, and OXA-48 β-lactamases display different substrate spectra, preliminary experiments were performed to choose a suitable antibiotic to compare the efficacy of the inhibitors (Figure 2). For each of the five chosen β-lactam/β-lactamase combinations, β-lactamase production led to large MIC increases, ranging from 256 to 4,096 fold. For the cefamandole/TEM-1 combination for example, production of TEM-1 in the *E. coli* Top10 host resulted in a 1,024-fold increase in the MIC of cefamandole (from 2 to 2,048 μg/ml) (Table 2). Such a high dynamic range offers the possibility to compare inhibitors with various efficacies leading to partial inhibition of the β-lactamases and various MICs in the 2 to 2,048 μg/ml range. Complete *in vivo* inhibition of TEM-1 requires very efficacious DBOs able to lead to the 1,024-fold decrease in the MIC needed to restore full susceptibility. For such inhibitors, the MICs of cefamandole against *E. coli* TOP10 and its isogenic TEM-producing derivative should be the same (2 μg/ml). For TEM-1 and cefamandole, this is the case for the first-generation inhibitor clavulanate (Table 2).

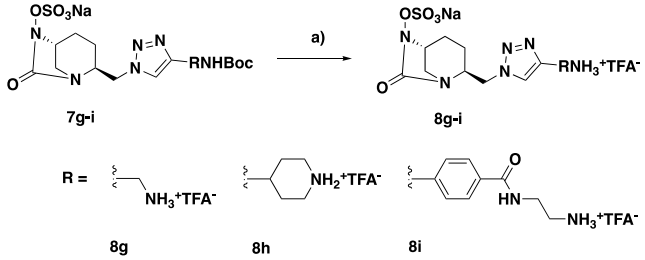

Scheme 4. a) TFA, DCM, 0°C, 1 h; **8g** (36%); **8h** (34%); **8i** (17%).

Rationale for *in vitro* evaluation of DBOs. Genes encoding soluble fragments of TEM-1, KPC-2, CTX-M-15, AmpC, and OXA-48 were cloned into the pET-TEV vector. β-lactamases were produced in *E. coli* BL21 and purified from clarified lysates by metal affinity and size-exclusion chromatography. For *in vitro* evaluation of inhibition efficacy, purified β-lactamases were incubated with DBOs at various concentrations with a fixed concentration of the chromogenic cephalosporin nitrocefin (Figure 3).[7] Estimates of the inhibition efficacy were provided by the ratio of the kinetic constants k_2 and K_i, which takes into account the first order constant k_2 for the chemical step of the reaction (carbamoylation) and the dissociation constant K_i for the preceding formation of a non-covalent complex.

Efficacy of inhibition of penicillinase TEM-1 by DBOs. The two reference DBOs, avibactam and relebactam, afforded

1,024- and 512-fold reductions in the MIC of cefamandole indicating that inhibition of TEM-1 was complete or nearly complete, respectively. Our synthetic DBOs offered the possibility to investigate the impact of aromatic rings, carboxylic acids, amines, and the corresponding Boc-protected compounds on the efficacy of DBOs. Two amine-containing compounds, **8g** and **8h**, were as active as relebactam, also producing a 512-fold reduction in the MIC of cefamandole. A 256-fold reduction was observed for compounds **7a** and **7f**, which contain a pyridine or a morpholine group in their side chain, respectively. The *in vivo* efficacy of the remaining compounds was lower, in particular that of Boc-protected compounds **7g**, **7h**, and **7i** (4- or 8-fold reduction in the MIC). The *in vitro* efficacy (k_2/K_i) of the latter compounds was in the 1,600 to 3,700 M^{-1} s^{-1} range. These values are similar to those of DBOs **8g**, **8h**, and **8i** (3,100 to 3,700 M^{-1} s^{-1} range) that afforded a 512-fold reduction in the MICs of cefamandole. The difference between the antibacterial activity of the two series of compounds (**7g**-**7i** *versus* **8g**-**8i**) may therefore result from a poor penetration of the Boc-containing compounds though the outer membrane of the tested strain. To further investigate the impact of the functionalization of the triazole ring, we synthesized regioisomers **10a** and **10b** containing unsubstituted triazoles. The inactivation efficacy of these compounds (k_2/K_i of 2,600 and 1,200 M^{-1} s^{-1}, respectively) was similar to that of compounds containing a substituted triazole ring (up to 4,700 M^{-1} s^{-1}), but *ca*. 19- and 9-fold lower than that of avibactam (88,000 M^{-1} s^{-1}) and relebactam (43,000 M^{-1} s^{-1}). These results indicate that the triazole linkage is disfavored in comparison to the carboxamide of avibactam or to the amide of relebactam. None of the tested side chains fully compensated this effect *in vitro*.

Efficacy of carbapenemase inhibition by DBOs. KPC-2 was fully inhibited by the two reference DBOs, avibactam and relebactam, affording a 4,096-fold reduction in the MIC of aztreonam used as the reporter drug for this β-lactamase (Table 3). Clavulanate was inactive as expected.[24] Among the DBOs synthesized in this study, **7a**, **7f**, **8g**, and **8h** were the most active *in vivo*, affording a 64-fold reduction in the MIC of aztreonam. However, the MIC of aztreonam in the presence of these inhibitors (MIC = 32 μg/ml) was much higher than that obtained with avibactam and relebactam (MIC = 0.5 μg/ml) indicating that KPC-2 retained substantial hydrolytic activity when the inhibitors were added to the culture medium. The difference in the MICs conveyed by **7a**, **7f**, **8g**, and **8h** in comparison to avibactam and relebactam correlated with a >20-fold lower inhibition efficacy *in vitro* (k_2/K_i in the 120 to 550 M^{-1} s^{-1} range for **7a**, **7f**, **8g**, and **8h** *versus* 26,000 and 10,000 M^{-1} s^{-1} for avibactam and relebactam, respectively). Comparisons of the data obtained with DBOs containing unsubstituted triazole rings (**10a** and **10b**; k_2/K_i of 350 and 280 M^{-1} s^{-1}, respectively) indicate that the side chain of three DBOs, **7a**, **7b,** and **7i** had a favorable impact on the inactivation efficacy (k_2/K_i of 550, 930, and 1,100 M^{-1} s^{-1}, respectively). Several side chains were poorly tolerated by KPC-2, including a trimethylsilyl in **7c** (k_2/K_i = 97 M^{-1} s^{-1}), a methoxy in **7d** (18 M^{-1} s^{-1}), and a carboxylate in **7j** (70 M^{-1} s^{-1}).

Efficacy of extended-spectrum β-lactamase inhibition by DBOs. Inhibition of CTX-M-15 was tested with amoxicillin as the reporter drug (Table 3). Avibactam fully inhibited CTX-M-15 *in vivo* (MIC = 2 μg/ml) but CTX-M-15 retained partial activity in bacteria exposed to relebactam (MIC = 16 μg/ml). In comparison with unsubstituted DBOs **10a** and **10b** (k_2/K_i of 120 and 280 M^{-1} s^{-1}, respectively), the pyridine and phenyl groups present in **7a**, **7b**, and **7i** enhanced CTX-M-15 inactivation (k_2/K_i of 1,700, 6,900, and 2,400 M^{-1} s^{-1}, respectively). However, these compounds displayed >18-fold lower *in vitro* efficacies in comparison to avibactam and, accordingly, **7a** and **7b** did not fully restore the antibacterial activity of amoxicillin (MIC of 32 and 64 μg/ml, respectively). Relebactam was less active than **7a** and **7b** *in vitro* (960 *versus* 1,700 and 6,900 M^{-1} s^{-1}). Accordingly, relebactam failed to fully inhibit CTX-M-15 *in vivo* (MIC = 16 μg/ml). DBO **7i** only afforded an 8-fold reduction in the MIC of amoxicillin in agreement with the proposed negative impact of the Boc group on permeability described

Table 1. Structure of alkynes used for CuAAC, resulting triazole-containing DBOs, and final sulfated compounds

Alkyne 5a-j		Compounds 6a-j			Compounds 7a-j		
5a	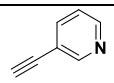	**6a**	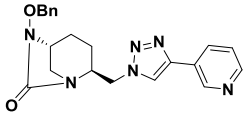	**(86%)**	**7a**	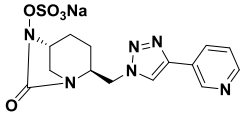	**(21%)**
5b	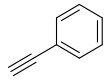	**6b**	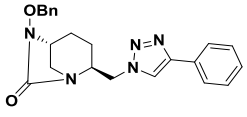	**(85%)**	**7b**	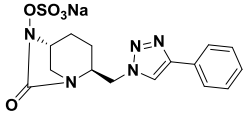	**(19%)**
5c		**6c**	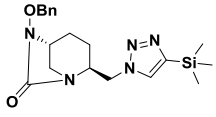	**(30%)**	**7c**	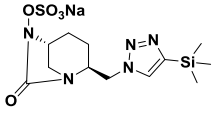	**(14%)**
5d	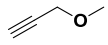	**6 d**	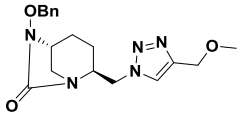	**(86%)**	**7d**	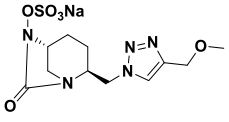	**(13%)**
							(18%)

5e	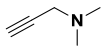	**6e**	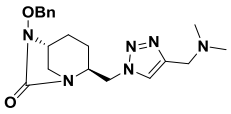	**(87%)**	**7e** 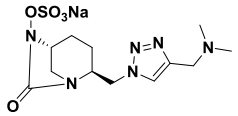
5f	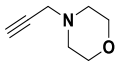 **(37%)**	**6f**	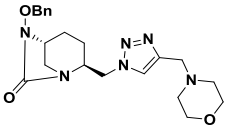	**(90%)**	**7f** 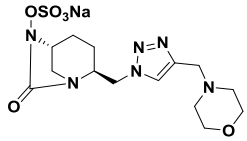 **(8%)**
5g	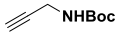 **(55%)**	**6g**	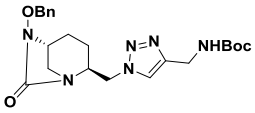	**(93%)**	**7g** 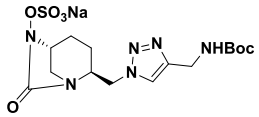
5h	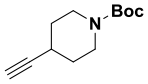	**6h**	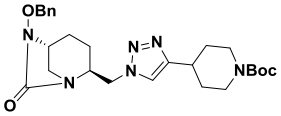	**(97%)**	**7h** 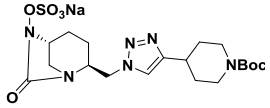 **(53%)**
5i	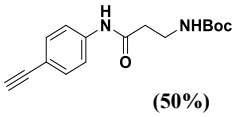 **(50%)**	**6i**	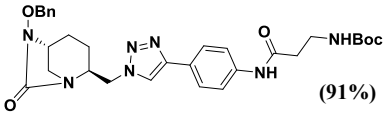	**(91%)**	**7i** 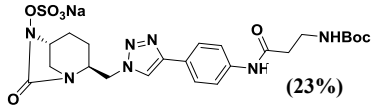 **(23%)**
5j	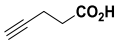	**6j**	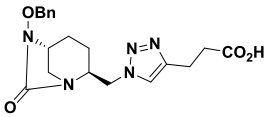	**(75%)**	**7j** 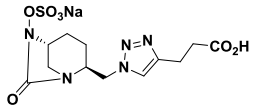 **(17%)**

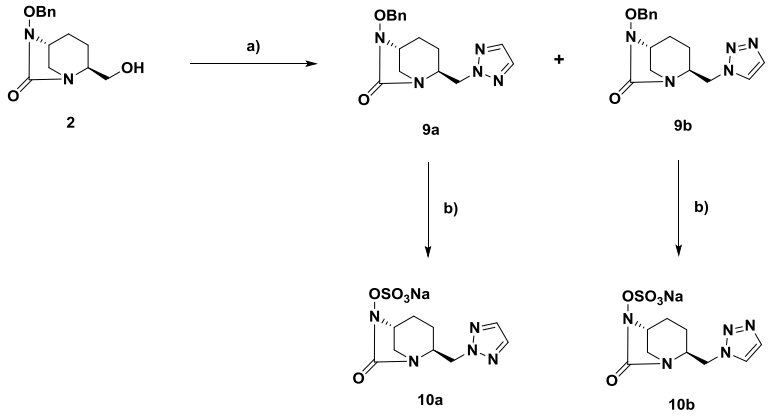

Scheme 5. a) i. MsCl, NEt_3, DMAP, DCM, 0°C, 1h, ii. 1H-1,2,3-triazole, tBuOK, MeCN, reflux, 15h; **9a** (44%); **9b** (37%); b) i. Pd/C, H_2, MeOH, rt, 48h, ii. SO_3-Pyr, pyridine, rt, overnight, iii. DOWEX Na^+; **10a** (27%); **10b** (8%).

above. Of note, four DBOs (avibactam, relebactam, **7a** and **7j**) slightly increased (4-fold) the activity of amoxicillin against the *E. coli* TOP10 host, which does not produce CTX-M-15. These results suggest that these DBOsmay inhibit PBP targets in addition to the β-lactamase. This would imply that the DBOs and amoxicillin may inhibit the targets in a cooperative manner leading to a higher antibacterial activity in comparison to amoxicillin alone. Of note, inhibition of class B PBP2 has been documented for several DBOs.[12, 13]

Inhibition of class C and D β-lactamases by DBOs. Production of AmpC in the *E. coli* Top10 host led to a 2,048-fold increase in the MIC of cefotaxime (from 0.125 to 256 μg/ml). *In vivo* inhibition of AmpC (class C) was partial for avibactam (MIC = 1 μg/ml) and nearly complete for relebactam (MIC = 0.25 μg/ml). The DBOs synthesized in this study achieved moderate MIC reduction and their *in vitro* inhibition efficacy was *ca*. 100-fold lower than that of the reference DBOs (avibactam and relebactam). The largest fold reductions in the MICs were obtained with **10a** and **10b** containing an unsubstituted triazole ring (from 256 to 32 and 16 μg/ml, respectively). Accordingly, these two compounds were the most active *in vitro* (200 and 210 M^{-1} s^{-1}) indicating that none of the side chains had a positive impact on inhibition efficacy. DBOs **7b** and **7i** were as active *in vitro* as DBOs **10a** and **10b** containing unsubstituted triazole rings. The side chain of other compounds had a negative impact leading to 5- to 13-fold lower inhibition efficacies.

Avibactam was the only DBO that significantly reduced the MIC of ertapenem against *E. coli* Top10 producing class D OXA-48 although the drug retained substantial antibacterial activity (MIC = 0.5 μg/ml *versus* < 0.03 μg/ml in the absence of OXA-48 production). *In vitro* evaluation indicated that four DBOs (**7b**, **7g**, **7h**, and **7i**) inhibited OXA-48 with efficacies similar to those of compounds **10a** and **10b**, which contained unsubstituted triazole rings (k_2/K_i ranges of 110 to 210 *versus* 140 to 150 M^{-1} s^{-1}, respectively). The side chains of other DBOs, including that of relebactam, were detrimental since no inhibition was detected at the highest concentration that was tested (100 μM).

Role of asparagine 132 in the carbamoylation efficacy of KPC-2 and CTX-M-15 by DBOs. The crystal structure of KPC-2 and CTX-M-15 acylated by avibactam revealed hydrogen interaction between the oxygen of the avibactam carboxamide group and the amine in the carboxamide group of Asn at position 132 of the β-lactamases (Ambler numbering) (Figure 4).[10, 25, 26] To assess the role of this interaction, we introduced the $N^{132}G$ substitution in KPC-2 and CTX-M-15 and determined the impact of the substitution on the carbamoylation efficacy of the β-lactamases by avibactam and **10b** (unsubstituted triazole) and **7b** (a phenyl-substituted triazole). Introduction of $N^{132}G$ in KPC-2 and CTX-M-15 was associated with large decreases in the avibactam carbamoylation efficacy (Table 5).

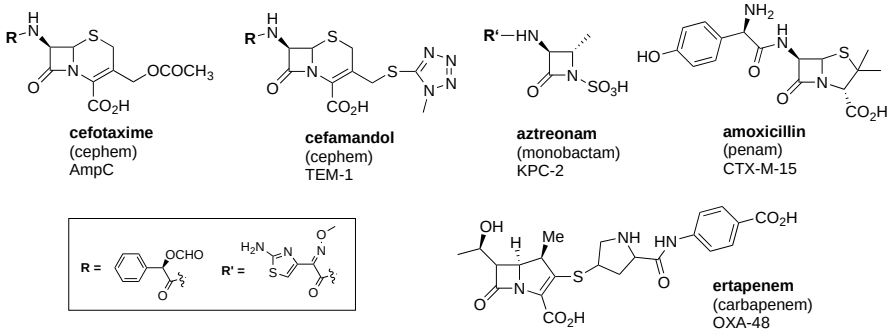

Figure 2. Structure of β-lactam antibiotics used as substrates to determine the activity of β-lactamases TEM-1, KPC-2, CTX-M-15, AmpC, and OXA-48. The drugs belong to the cephem, monobactam, penam, or carbapenem classes of β-lactams, as indicated in parenthesis.

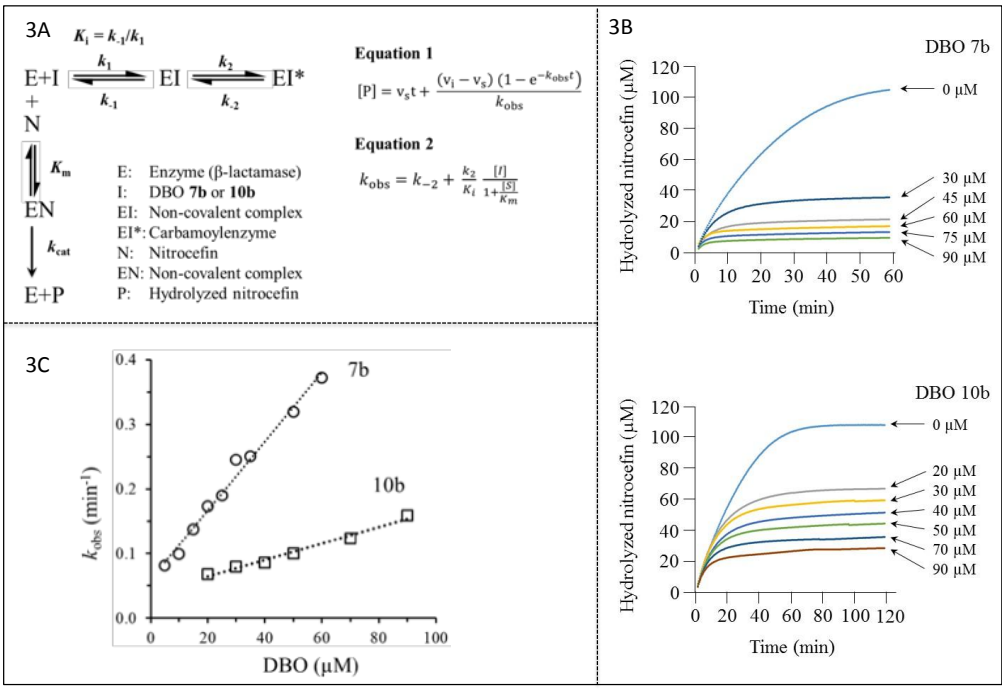

Figure 3. Inhibition of β-lactamases by DBOs. (A) Reaction scheme and definition of rate constants. v_i and v_s are the initial and final velocities of the reactions. (B) Time-dependent inhibition of KPC-2 by **7b** and **10b**. KPC-2 (2.5 nM) was incubated with nitrocefin (100 μM) and various concentrations of **7b** and **10b** (20-90 μM or 30-90 μM, respectively). Equation 1 was fitted to progress curves to obtain the pseudo-first order rate constant k_{obs}. (C) Determination of carbamoylation rate constant k_2/K_i. k_{obs} was plotted as a function of the DBO concentration. Equation 2 was fitted to data to determine the value of the k_2/K_i ratio and of k_{-2}. Kinetic constant k_{-2} was low for all DBOs (See supplementary Table S1).

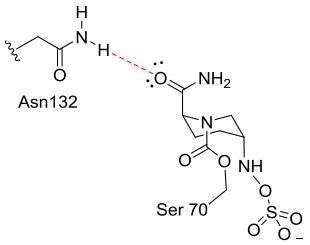

Figure 4. Hydrogen interaction between the carboxamides of avibactam and Asn at position 132 of β-lactamases (Ambler numbering).

In comparison, the substitution had a lower impact on the efficacy of carbamoylation of KPC-2 and CTX-M-15 by **10b** and **7b**. The latter compounds were much less active than avibactam against the wild-type enzymes but as active as avibactam against KPC-2 and CTX-M-15 harboring $N^{132}G$. These observations suggest that the hydrogen interaction between avibactam and N^{132} is critical for efficacious carbamoylation of KPC-2 and CTX-M-15 by avibactam and that the absence of this interaction in the case of triazole-containing DBOs could be largely responsible for their lower efficacy in comparison to avibactam. The modest k_2/K_i reductions observed for **10b** and **7b** following introduction of $N^{132}G$ could be accounted for by additional roles of N^{132} or a weak interaction of the latter residue with the triazole ring. The role of the hydrogen interaction involving N^{132} is also highlighted by comparison of relebactam and compound **8h** that contain the same side chain connected to the DBO scaffold by an amide or triazole, respectively.

Conclusions. Efficacies of the 17 DBOs for inhibition of TEM-1, KPC-2, CTX-M-15, AmpC, and OXA-48 were recapitulated in a heat map (Figure 5A) to highlight key differences. Compounds **10a** and **10b**, containing unsubstituted triazole rings, were less active than the reference DBOs (avibactam and relebactam) against TEM-1, KPC-2, CTX-M-15, and AmpC. Loss of the hydrogen interaction between the carboxamide of avibactam and conserved residue N^{132} is likely to be responsible for reduced activity that could not be fully compensated by any of the substituents introduced in the triazole ring. In comparison to **10a** and **10b**, two DBOs, **7a** and **7b**, displayed improved inhibition efficacies, in particular against the KPC-2 carbapenemase and the CTX-M-15 extended-spectrum β-lactamase, indicating that the pyridine and phenyl groups present in **7a** and **7b** had a positive impact on the inhibition of these class A β-lactamases. Several side chains had a deleterious effect, in particular the methoxy and carboxyl groups present in **7d** and **7j**. *In vivo* antibacterial susceptibility data were recapitulated in a heat map presented in Figure 5B. The most active DBOs *in vitro* (**7a** and **7b**) were

Table 5. Impact of the $N^{132}G$ substitution on the cabamoylation efficacy (k_2/K_i) of KPC-2 and CTX-M-15

by DBOs

β-lactamase	k_2/K_i (M^{-1} s^{-1}) for indicated DBO		
	Avibactam	10b	7b
KPC-2	26,000 ± 1,000	280 ± 30	930 ± 40
KPC-2 $N^{132}G$	53 ± 3	31 ± 6	21 ± 3
CTX-M-15	130,000 ± 10,000	280 ± 10	6,900 ± 200
CTX-M-15 $N^{132}G$	70 ± 6	6.6 ± 2.0	140 ± 10

also among the most active compounds for restoring the activity of β-lactams against KPC-2- or CTX-M-15-producing *E. coli* strains. The correlation between antibacterial activity and *in vitro* inhibition efficacies did not appear to apply to all DBOs, in particular for DBOs containing protected amines, which appeared to be less active *in vivo* than expected from their *in vitro* activity. This was explored by plotting the *in vitro* efficacy of the DBOs against the fold reduction of the MICs they afforded (Figure 6A). Plotting the complete set of data, *i.e.* the inhibition of five β-lactamases by 17 DBOs, revealed a positive correlation between the Log_{10} of the inhibition efficacy (Log_{10} of k_2/K_i) and the Log_2 of the fold reduction in the MIC of the reporter drugs (Spearman correlation coefficient of 0.72; $p = 5.3\ 10^{-14}$). DBOs harboring a Boc group in their side chain clustered below the regression line indicating that their *in vitro* efficacy was not translated into antibacterial activity due to impaired penetration through the outer membrane (Figure 6B). The Spearman correlation coefficient calculated without Boc-containing compounds was higher than that calculated with the entire set of data (0.87; $p = 4.7\ 10^{-21}$). In contrast, amine-containing compounds clustered above the regression line indicating a facilitated access to the periplasm (Figure 6C).

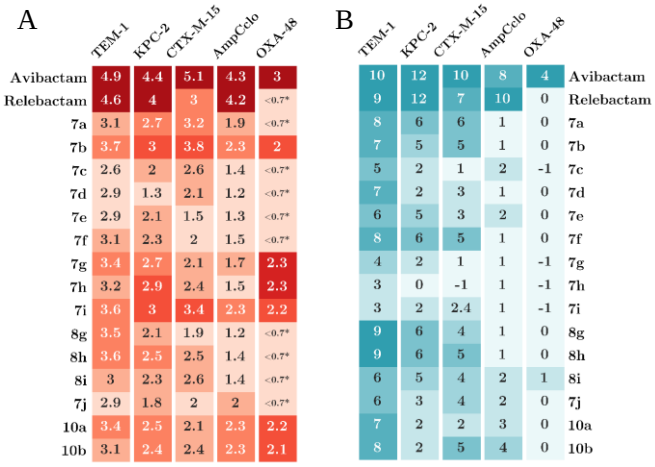

Figure 5. Heat maps highlighting differences in (A) the efficacy of *in vitro* inhibition of β-lactamases (Log_{10} of k_2/K_i) and (B) the antibacterial activity (Log_2 of the fold reduction in the MICs). *: No inhibition at the highest inhibitor concentration that was tested (100 μM). The color code shows the activities relative to the most active compound for each β-lactamase.

To summarize, we have developed an efficient strategy based on copper(I)-catalyzed Huisgen-Sharpless cycloaddition reaction for the synthesis of new DBOs. To achieve this goal, an improvement of the original synthesis of azido derivative **4** has been realized. Our methodology is compatible with a wide range of functional groups for the modification of the C2 position of the DBO scaffold. The synthetic route provides a versatile approach to explore the chemical space for novel interactions with the catalytic cavity of potential targets[3, 12, 13, 21] although the first series of triazole-containing compounds reported in this study did not lead to inhibitors with improved characteristics for inhibition of β-lactamases of Gram-negative bacteria. The reduced efficacy could be due to the absence of hydrogen bonding with a conserved asparagine residue at position 132. This could only be partially compensated by additional interactions involving the triazole substituents.

General procedures. Reactions were carried out under argon atmosphere and solvents were dried using standard methods and distilled before use. Unless otherwise specified, materials were purchased from commercial suppliers and used without further purification. TLC was performed using Merck commercial aluminum sheets coated with silica gel 60 F_{254}. Compounds were detected by charring with phosphomolibdic acid in ethanol followed by heating. Purification was performed by flash chromatography on silica gel (60 Å, 180-240 mesh; Merck) or by preparative high-performance liquid chromatography (HPLC) using Shimadzu Prominence system with a Zorbax Extend-C18 prepHT column (150 x 21.2 mm, 5 μm; Agilent). Compounds were eluted with a linear gradient (from 100% of H_2O to 100% of CH_3CN) that was applied between 5 and 30 min at a flow rate of 15 ml/min. Products were detected by UV absorption at 214 nm. NMR spectra were recorded on Bruker spectrometers (AM250, Avance II 500 and Avance III HD 4000). Chemical shifts (δ) are reported in ppm and referenced to the residual proton or carbon resonance of the solvents: $CDCl_3$ (δ 7.26), D_2O (δ 4.79) or $(CD_3)_2SO$ (δ 2.50) for ^1H and $CDCl_3$ (δ 77.16) or $(CD_3)_2SO$ (δ 39.52) for ^{13}C. Signals were assigned using 1D (^1H and ^{13}C) and 2D (HSQC, COSY, and HMBC) spectra. NMR coupling constants (J) are reported in hertz (Hz). High-resolution mass spectroscopy (HRMS) was recorded with an ion trap mass analyzer under electrospray ionization (ESI) in the negative or positive ionization detection mode. HRMS was performed using Thermo Scientific LTQ Orbitrap XL and Bruker MaXis II ETD spectrometers. The purity of final compounds (≥95%) was etablished by analytical HPLC, which was performed on a Shimadzu Prominence system with a Hypersil® BDS C18 column (150 x 4.6 mm, 5 μm) or an Agilent Zorbax Extend C18 column (250 x 4.6 mm, 5 μm) with UV detection at 214 and 220 nm. Optical rotations were measured with a sodium lamp (589 nm) at 20°C on a Perkin Elmer polarimeter.

Compound 4. Isobutyl chloroformate (6.26 ml, 47.1 mmol) was added dropwise at 0°C to a solution of (2S,5R)-6-(benzyloxy)-7-oxo-1,6-diazabicyclo[3.2.1]octane-2-carboxylic acid **1** (6.5 g, 23.5 mmol) and triethylamine (3.64 ml, 25.9 mmol) in THF (75 ml). The solution was stirred at 0°C for 2 h and $NaBH_4$ (2.72 g, 70.6 mmol) was gradually added. The reaction mixture was stirred for 3 additional hours at 0°C. Water (110 ml) and ethyl acetate (110 ml) were slowly added and the heterogeneous mixture was stirred for 30 min at room temperature. The organic layer was washed with brine, dried over $MgSO_4$, and concentrated under reduced pressure

to afford (2S,5R)-6-(benzyloxy)-2-(hydroxymethyl)-1,6-diazabicyclo[3.2.1]octan-7-one **2**, which was used in the next step without further purification. Triethylamine (9.94 ml, 70.6 mmol), DMAP (4.36 g, 35.3 mmol) and MsCl (2.76 ml, 35.3 mmol) were added at 0°C to a solution of crude product **2** (23.5 mmol) in DCM (71 ml). The reaction mixture was stirred at 0°C for 2 h. DCM was then added and the organic layer was washed with brine, dried over $MgSO_4$, and concentrated under vacuum to afford ((2S,5R)-6-(benzyloxy)-7-oxo-1,6-diazabicyclo[3.2.1]octan-2-yl)methyl methanesulfonate **3**, which was used in the next step without further purification. Sodium azide (7.69 g, 117 mmol) was added to a solution of ((2S,5R)-6-(benzyloxy)-7-oxo-1,6-diazabicyclo[3.2.1]octan-2-yl)methyl methanesulfonate **3** (23.5 mmol) in DMF (95 ml). The solution was stirred at 90°C for 20 h. After being cooled to room temperature, ethyl acetate was added and the organic layer was washed with brine, dried over $MgSO_4$, and concentrated under reduced pressure. Purification by flash chromatography using cyclohexane/ethyl acetate (7/3) as the eluent gave compound **4** as a white solid (2.4 g, 35% over 3 steps). ^{1}H NMR (500 MHz, $CDCl_3$) δ 7.43 - 7.33 (m, 5H, $H_{10, 11, 12}$), 5.04 (d, *J* = 11.5 Hz, 1H, H_8), 4.89 (d, *J* = 11.5 Hz, 1H, H_8), 3.61 – 3.56 (m, 1H, H_1), 3.53 (dd, *J* = 12.5, 7.4 Hz, 1H, H_7), 3.35 – 3.32 (m, 2H, $H_{4, 7}$), 2.97 (s, 2H, H_5), 2.06 – 2.02 (m, 1H, H_3), 2.01 – 1.95 (m, 1H, H_2), 1.63 – 1.55 (m, 1H, H_3), 1.54 – 1.49 (m, 1H, H_2). ^{13}C NMR (125 MHz, $CDCl_3$) δ 169.7 (C_6), 136.0 (C_9), 129.3 (C_{11}), 128.8 (C_{12}), 128.6 (C_{10}), 78.3 (C_8), 58.6 (C_4), 56.6 (C_1), 53.3 (C_7), 44.1 (C_5), 20.5 (C_2), 20.0 (C_3). HRMS calculated for $C_{14}H_{18}N_5O_2$ $[M+H]^+$: 288.14605; found 288.14523. $[\alpha]_D$: –53.2° (7.8 mg/ml, MeOH).

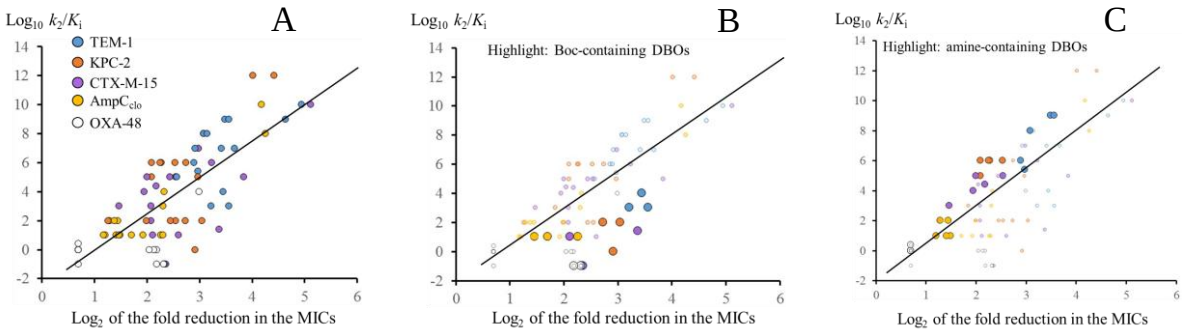

Figure 6. Correlation between the efficacy of DBOs in reducing MICs and in inhibiting β-lactamases. The trend line was obtained by linear regression. (A) Complete set of data. (B) The regression line was calculated by omitting Boc-containing DBOs (highlighted with large circles). (C) Clustering of amine-containing DBOs above the regression line (highlighted with large circles).

General procedure for Copper(I)-catalyzed azide-alkyne cycloaddition reaction. To a solution of azido **4** in THF, were successively added alkyne **5** (2 eq), sodium ascorbate (0.6 eq, in water) and $CuSO_4$ (0.3 eq, in water). The heterogeneous mixture was stirred overnight at room temperature. Ethyl acetate was added and the organic layer was washed with brine, dried over $MgSO_4$, and concentrated under reduced pressure. The crude product was purified by flash chromatography to afford product **6**.

General procedure for introduction of sodium sulphite. 10 wt. % Pd/C (1 eq) was added to a solution of **6** in MeOH and the reaction mixture was stirred under H_2 for 48 h at room temperature. Palladium was removed by filtration through celite and the filtrate concentrated. Sulfur trioxide pyridine complex (6 eq) was added to a solution of deprotected compound in pyridine and the reaction mixture was stirred for 2 h at room temperature. Additional SO_3-pyridine complex (2 eq) was added, stirred overnight at room temperature, and pyridine was removed under reduced pressure. The crude product was solubilized in water, filtered, eluted on Dowex-Na resin with H_2O, and lyophilized. The residue was dissolved in EtOH, filtered, and concentrated under vacuum. HPLC purification afforded product **7.**

General procedure for Boc deprotection. TFA (12 eq) was added dropwise at 0°C to a solution of **7** (1 eq) in DCM. The reaction mixture was stirred at 0°C for 1 h and concentrated under vacuum. HPLC purification afforded product **8**.

Compound 6a. Following the general procedure for CuAAC, starting from compound **4** (200 mg, 0.70 mmol) and 3-ethynylpyridine **5a** (144 mg, 1.39 mmol), and using DCM/MeOH (96/4) as eluent for flash chromatography purification, compound **6a** was obtained as a colorless oil (234 mg, 86%). ^{1}H NMR (500 MHz, $CDCl_3$) δ 9.01 (bs, 1H, H_{14}), 8.57 (bd, *J* = 3.8 Hz, 1H, H_{13}), 8.17 (dt, *J* = 7.9, 2.0 Hz, 1H, H_{11}), 8.05 (s, 1H, H_8), 7.42 – 7.33 (m, 6H, $H_{12, 17, 18, 19}$), 5.02 (d, *J* = 11.5 Hz, 1H, H_{15}), 4.88 (d, *J* = 11.5 Hz, 1H, H_{15}), 4.62 (dd, *J* = 14.3, 8.3 Hz, 1H, H_7), 4.56 (dd, *J* = 14.3, 6.5 Hz, 1H, H_7), 3.92 – 3.87 (m, 1H, H_1), 3.38 – 3.36 (m, 1H, H_4), 2.99 – 2.92 (m, 2H, H_5), 2.12 – 2.07 (m, 1H, H_3), 2.06 – 1.99 (m, 1H, H_2), 1.73 – 1.67 (m, 1H, H_3), 1.65 – 1.59 (m, 1H, H_2). ^{13}C NMR (125 MHz, $CDCl_3$) δ 169.4 (C_6), 149.4 (C_{13}), 147.3 (C_{14}), 145.3 (C_9), 135.8 (C_{16}), 133.2 (C_{11}), 129.4 (C_{18}), 128.9 (C_{19}), 128.7 (C_{17}), 126.8 (C_{10}), 123.9 (C_{12}), 120.5 (C_8), 78.4 (C_{15}), 58.4 (C_4), 56.7 (C_1), 52.1 (C_7), 43.8 (C_5), 20.5 (C_2), 19.8 (C_3). HRMS calculated for $C_{21}H_{23}N_6O_2$ $[M+H]^+$: 391.18825; found: 391.18886. $[\alpha]_D$: –17.9° (8.0 mg/ml, MeOH).

Compound 6b. Following the general procedure for CuAAC, starting from compound **4** (200 mg, 0.70 mmol) and phenylacetylene **5b** (154 µl, 1.40 mmol), and using cyclohexane/ethyl acetate (4/6) as eluent for flash chromatography purification, compound **6b** was obtained as a colorless oil (232 mg, 85%). ^{1}H NMR (500 MHz, $CDCl_3$) δ 7.97 (s, 1H, H_8),

7.83 (d, J = 7.2 Hz, 2H, H_{11}), 7.43 – 7.32 (m, 8H, $H_{12, 13, 16, 17, 18}$), 5.03 (d, J = 11.5 Hz, 1H, H_{14}), 4.88 (d, J = 11.5 Hz, 1H, H_{14}), 4.63 – 4.54 (m, 2H, H_7), 3.91 – 3.86 (m, 1H, H_1), 3.36 – 3.35 (m, 1H, H_4), 2.97 – 2.90 (m, 2H, H_5), 2.10 – 2.06 (m, 1H, H_3), 2.03 – 1.96 (m, 1H, H_2), 1.72 – 1.68 (m, 1H, H_3), 1.66 – 1.60 (m, 1H, H_2). ^{13}C NMR (125 MHz, $CDCl_3$) δ 169.3 (C_6), 148.2 (C_9), 135.8 (C_{15}), 130.3 (C_{10}), 129.4 (C_{17}), 129.0 (C_{12}), 128.9 (C_{18}), 128.7 (C_{16}), 128.5 (C_{13}), 126.0 (C_{11}), 120.3 (C_8), 78.4 (C_{14}), 58.4 (C_4), 56.7 (C_1), 52.2 (C_7), 43.9 (C_5), 20.4 (C_2), 19.8 (C_3). HRMS calculated for $C_{22}H_{24}N_5O_2$ $[M+H]^+$: 390.19300; found: 390.19165. $[\alpha]_D$: −44.5° (5.2 mg/ml, DMSO).

Compound 6c. Following the general procedure for CuAAC, starting from compound **4** (200 mg, 0.70 mmol) and ethynyltrimethylsilane **5c** (388 µl, 2.80 mmol), and using cyclohexane/ethyl acetate (3/7) as eluent for flash chromatography purification, compound **6c** was obtained as a colorless oil (82 mg, 30%). ^{1}H NMR (250 MHz, $CDCl_3$) δ 7.64 (s, 1H, H_8), 7.42 – 7.32 (m, 5H, $H_{13, 14, 15}$), 5.01 (d, J = 11.5 Hz, 1H, H_{11}), 4.86 (d, J = 11.5 Hz, 1H, H_{11}), 4.55 (d, J = 7.3 Hz, 2H, H_7), 3.85 – 3.75 (m, 1H, H_1), 3.34 – 3.30 (m, 1H, H_4), 2.95 – 2.82 (m, 2H, H_5), 2.09 – 1.97 (m, 1H, H_3), 1.96 – 1.85 (m, 1H, H_2), 1.72 – 1.62 (m, 1H, H_3), 1.62 – 1.50 (m, 1H, H_2), 0.30 (s, 9H, H_{10}). ^{13}C NMR (125 MHz, $CDCl_3$) δ 169.6 (C_6), 147.3 (C_9), 135.9 (C_{12}), 129.4 (2C, C_8 and C_{14}), 128.9 (C_{15}), 128.7 (C_{13}), 78.4 (C_{11}), 58.5 (C_4), 56.8 (C_1), 51.5 (C_7), 44.0 (C_5), 20.3 (C_2), 19.9 (C_3), -1.0 (C_{10}). HRMS calculated for $C_{19}H_{28}N_6O_2Si$ $[M+H]^+$: 386.20123; found: 386.20053. $[\alpha]_D$: −24.4° (5.6 mg/ml, MeOH).

Compound 6d. Following the general procedure for CuAAC, starting from compound **4** (200 mg, 0.70 mmol) and methyl propargyl ether **5d** (118 µl, 1.40 mmol), and using DCM/MeOH (96/4) as eluent for flash chromatography purification, compound **6d** was obtained as a colorless oil (215 mg, 86%). ^{1}H NMR (500 MHz, $CDCl_3$) δ 7.70 (s, 1H, H_8), 7.42 – 7.33 (m, 5H, $H_{14, 15, 16}$), 5.02 (d, J = 11.5 Hz, 1H, H_{12}), 4.87 (d, J = 11.5 Hz, 1H, H_{12}), 4.57 (s, 2H, H_{10}), 4.55 – 4.48 (m, 2H, H_7), 3.81 (qd, J = 7.4, 4.2 Hz, 1H, H_1), 3.40 (s, 3H, H_{11}), 3.34 (q, J = 3.0 Hz, 1H, H_4), 2.93

Table 2. Inhibition of penicillinase TEM-1 by DBOs and clavulanate

R =		Carbamoylation efficacy ($M^{-1} s^{-1}$)	MIC of cefamandole (µg/ml)	
			Without TEM-1	With TEM-1
no inhibitor		NA	2	2,048
	Avibactam	88,000 ± 2,000	2	2
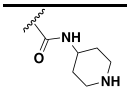	Relebactam	43,000 ± 1,000	2	4
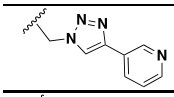	7a	1,400 ± 100	2	8
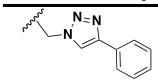	7b	4,700 ± 1,000	4	16
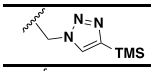	7c	370 ± 50	2	64
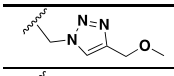	7d	830 ± 50	2	16
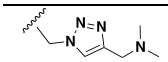	7e	780 ± 80	2	32
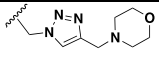	7f	1,200 ± 100	2	8
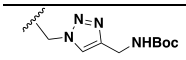	7g	2,800 ± 400	2	128
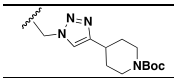	7h	1,700 ± 200	2	256
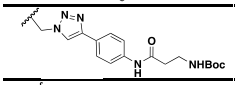	7i	3,700 ± 500	2	256
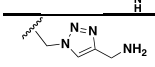	8g	3,100 ± 200	4	4
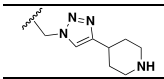	8h	3,600 ± 300	2	4
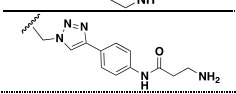	8i	940 ± 150	2	32

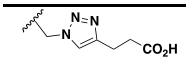	7j	720 ± 60	2	32
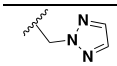	10a	2,600 ± 300	2	16
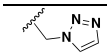	10b	1,200 ± 100	2	8
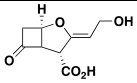	Clavulanate	NA	2	2

NA, not applicable as clavulanate and DBOs have different modes of action.

Table 3. Inhibition of class A β-lactamases by DBOs and clavulanate

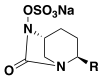 R =		Inhibition of KPC-2			Inhibition of CTX-M-15		
			MIC of aztreonam (μg/ml)			MIC of amoxicillin (μg/ml)	
		Carbamoylation efficacy ($M^{-1} s^{-1}$)	With-out KPC-2	With KPC-2	Carbamoylation efficacy ($M^{-1} s^{-1}$)	Without CTX-M-15	With CTX-M-15
no inhibitor		NA	0.5	2,048	NA	8	2,048
	Avibactam	26,000 ± 1,000	0.25	0.5	130,000 ± 10,000	2	2
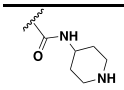	Relebactam	10,000 ± 1,000	0.25	0.5	960 ± 80	2	16
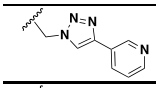	7a	550 ± 10	0.25	32	1,700 ± 400	2	32
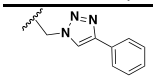	7b	930 ± 40	0.25	64	6,900 ± 2,000	8	64
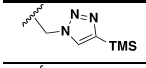	7c	97 ± 8	0.5	512	400 ± 10	8	1,024
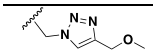	7d	18 ± 2	0.5	512	120 ± 40	8	256
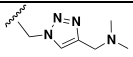	7e	120 ± 50	0.5	64	29 ± 5	4	256
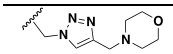	7f	190 ± 20	0.25	32	100 ± 10	8	64
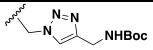	7g	540 ± 60	0.25	512	130 ± 10	8	1,024
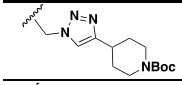	7h	830 ± 90	0.25	2,048	230 ± 30	8	4,096
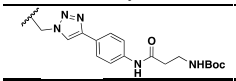	7i	1,100 ± 200	0.5	512	2,400 ± 200	8	768
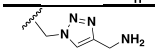	8g	120 ± 10	0.25	32	88 ± 13	4	128
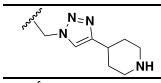	8h	340 ± 30	0.25	32	350 ± 60	4	64
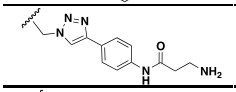	8i	180 ± 33	0.25	64	150 ± 10	4	128
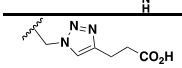	7j	70 ± 8	0.25	256	110 ± 10	2	96
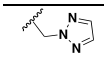	10a	350 ± 40	0.5	512	120 ± 10	4	512
	10b	280 ± 30	0.25	512	280 ± 10	8	64
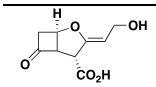	Clavulanate	NA	0.5	512	NA	8	2

NA, not applicable as clavulanate and DBOs have different modes of action.

Table 4. Inhibition of class C (AmpC) and class D (OXA-48) β-lactamases by DBOs and clavulanate

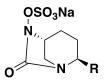 R =		Inhibition of AmpC			Inhibition of OXA-48		
			MIC of cefotaxime (μg/ml)			MIC of ertapenem (μg/ml)	
		Carbamoylation efficacy ($M^{-1} s^{-1}$)	With-out AmpC	With AmpC	Carbamoylation efficacy ($M^{-1} s^{-1}$)	Without OXA-48	With OXA-48
no inhibitor		NA	0.125	256	NA	< 0.03	8
	Avibactam	18,000 ± 1,000	0.125	1	980 ± 60	< 0.03	0.5
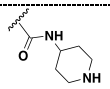	Relebactam	15,000 ± 2,000	0.125	0.25	No inhibition	< 0.03	8
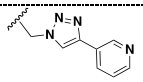	7a	85 ± 7	0.125	128	No inhibition	< 0.03	8
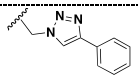	7b	200 ± 10	0.25	128	110 ± 30	< 0.03	8
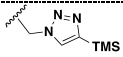	7c	24 ± 1	0.125	64	No inhibition	< 0.03	16
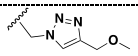	7d	15 ± 5	0.125	128	No inhibition	< 0.03	16
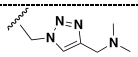	7e	20 ± 8	0.125	64	No inhibition	< 0.03	8
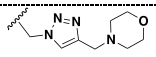	7f	31 ± 3	0.125	128	No inhibition	< 0.03	8
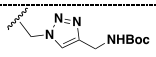	7g	51 ± 8	0.125	128	210 ± 50	< 0.03	16
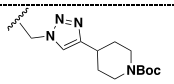	7h	29 ± 6	0.125	128	210 ± 30	< 0.03	16
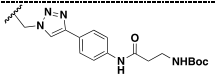	7i	180 ± 20	0.125	128	150 ± 40	< 0.03	16
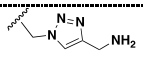	8g	16 ± 2	0.125	128	No inhibition	< 0.03	8
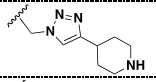	8h	26 ± 2	0.125	128	No inhibition	< 0.03	8
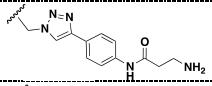	8i	28 ± 13	0.25	64	No inhibition	< 0.03	4
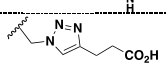	7j	99 ± 9	0.25	64	No inhibition	< 0.03	8
	10a	200 ± 20	0.125	32	150 ± 30	< 0.03	8
	10b	210 ± 20	0.125	16	140 ± 20	< 0.03	8
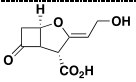	Clavulanate	NA	0.0625	128	NA	< 0.03	8

NA, not applicable as clavulanate and DBOs have different modes of action. No inhibition, no inhibition at the highest inhibitor concentration that was tested (100 μM).

(bd, J = 11.9 Hz, 1H, H_5), 2.88 (d, J = 11.9 Hz, 1H, H_5), 2.09 – 2.03 (m, 1H, H_3), 1.97 (dq, J = 15.1, 7.4 Hz, 1H, H_2), 1.70 – 1.63 (m, 1H, H_3), 1.60 – 1.54 (m, 1H, H_2). ^{13}C NMR (125 MHz, CDCl3) δ 169.4 (C_6), 145.8 (C_9), 135.9 (C_{13}), 129.4 (C_{15}), 128.9 (C_{16}), 128.7 (C_{14}), 123.0(C_8), 78.4 (C_{12}), 66.1 (C_{10}), 58.5 (C_{11}), 58.4 (C_4), 56.7 (C_1), 52.0 (C_7), 43.9 (C_5), 20.4 (C_2), 19.8 (C_3). HRMS calculated for $C_{18}H_{24}N_5O_3$ $[M+H]^+$: 358.18791; found: 358.218771. $[\alpha]_D$: −27.7° (6.6 mg/ml, MeOH).

Compound 6e. Following the general procedure for CuAAC, starting from compound **4** (150 mg, 0.52 mmol) and 3-dimethylamino-1-propyne **5e** (112 µl, 1.04 mmol), and using DCM/MeOH (9/1) + 1% NH_4OH as eluent for flash chromatography purification, compound **6e** was obtained as a pale yellow oil (169 mg, 87%). ^{1}H NMR (500 MHz, $CDCl_3$) δ 7.65 (s, 1H, H_8), 7.38 – 7.28 (m, 5H, $H_{14, 15, 16}$), 4.97 (d, J = 11.5 Hz, 1H, H_{12}), 4.83 (d, J = 11.5 Hz, 1H, H_{12}), 4.54 – 4.44 (m, 2H, H_7), 3.79 – 3.74 (m, 1H, H_1), 3.56 (s, 2H, H_{10}), 3.36 – 3.34 (m, 1H, H_4), 2.95 – 2.87 (m, 2H, H_5), 2.22 (s, 6H, H_{11}), 2.03 – 1.97 (m, 1H, H_3), 1.95 – 1.87 (m, 1H, H_2), 1.68 – 1.62 (m, 1H, H_3), 1.55 – 1.49 (m, 1H, H_2). ^{13}C NMR (125 MHz, $CDCl_3$) δ 169.4 (C_6), 143.3 (C_9), 135.9 (C_{13}), 129.4 (C_{15}), 128.9 (C_{16}), 128.7 (C_{14}), 124.2 (C_8), 78.4 (C_{12}), 58.4 (C_4), 56.9 (C_1), 53.9 (C_{10}), 52.0 (C_7), 44.5 (C_{11}), 43.7 (C_5), 20.4 (C_2), 19.8 (C_3). HRMS calculated for $C_{19}H_{27}N_6O_2$ $[M+H]^+$: 371.21955; found: 371.21900. $[\alpha]_D$: −24.7° (7.5 mg/ml, MeOH).

Compound 6f. Following the general procedure for CuAAC, starting from compound **4** (80 mg, 0.28 mmol) and compound **5f** (70 mg, 0.56 mmol), and using DCM/MeOH (96/4) as eluent for flash chromatography purification, compound **6f** was obtained as a colorless oil (104 mg, 90%). ^{1}H NMR (500 MHz, $CDCl_3$) δ 7.61 (s, 1H, H_8), 7.37 – 7.28 (m, 5H, $H_{15,16,17}$), 4.96 (d, J = 11.5 Hz, 1H, H_{13}), 4.83 (d, J = 11.5 Hz, 1H, H_{13}), 4.49 (dd, J = 14.2, 8.1 Hz, 1H, H_7), 4.44 (dd, J = 14.2, 6.9 Hz, 1H, H_7), 3.78 – 3.73 (m, 1H, H_1), 3.64 (t, J = 4.7 Hz, 4H, H_{12}), 3.60 (s, 2H, H_{10}), 3.33 (bs, 1H, H_4), 2.88 (s, 2H, H_5), 2.45 (t, J = 4.7 Hz, 4H, H_{11}), 2.03 – 1.98 (m, 1H, H_3), 1.95 – 1.87 (m, 1H, H_2), 1.66 – 1.60 (m, 1H, H_3), 1.54 – 1.48 (m, 1H, H_2). ^{13}C NMR (125 MHz, $CDCl_3$) δ 169.3 (C_6), 144.5 (C_9), 135.7 (C_{14}), 129.2 (C_{16}), 128.7 (C_{17}), 128.5 (C_{15}), 123.0 (C_8), 78.2 (C_{13}), 66.8 (C_{12}), 58.2 (C_4), 56.7 (C_1), 53.6 (C_{10}), 53.4 (C_{11}), 51.7 (C_7), 43.7 (C_5), 20.3 (C_2), 19.6 (C_3). HRMS calculated for $C_{21}H_{29}N_6O_3$ $[M+H]^+$: 413.22957; found: 413.22753. $[\alpha]_D$: −17.3° (4.4 mg/ml, MeOH).

Compound 6g. Following the general procedure for CuAAC, starting from compound **4** (200 mg, 0.70 mmol) and compound **5g** (217 mg, 1.40 mmol), and using cyclohexane/ethyl acetate (1/9) as eluent for flash chromatography purification, compound **6g** was obtained as a colorless oil (289 mg, 93%). ^{1}H NMR (500 MHz, $CDCl_3$) δ 7.62 (s, 1H, H_8), 7.39 – 7.30 (m, 5H, $H_{16, 17, 18}$), 4.98 (d, J = 11.5 Hz, 1H, H_{14}), 4.84 (d, J = 11.5 Hz, 1H, H_{14}), 4.51 (dd, J = 14.2, 8.1 Hz, 1H, H_7), 4.44 (dd, J = 14.2, 6.9 Hz, 1H, H_7), 4.34 (d, J = 5.9 Hz, 2H, H_{10}), 3.79 – 3.74 (m, 1H, H_1), 3.33 (bs, 1H, H_4), 2.89 (s, 2H, H_5), 2.05 – 1.99 (m, 1H, H_3), 1.97 – 1.89 (m, 1H, H_2), 1.67 – 1.60 (m, 1H, H_3), 1.54 – 1.48 (m, 1H, H_2), 1.41 (s, 9H, H_{13}). ^{13}C NMR (125 MHz, $CDCl_3$) δ 169.3 (C_6), 155.9 (C_{11}), 145.9 (C_9), 135.8 (C_{15}), 129.3 (C_{17}), 128.8 (C_{18}), 128.6 (C_{16}), 122.3 (C_8), 79.7 (C_{12}), 78.2 (C_{14}), 58.3 (C_4), 56.7 (C_1), 51.7 (C_7), 43.8 (C_5), 36.3 (C_{10}), 28.4 (C_{13}), 20.3 (C_2), 19.7 (C_3). HRMS calculated for $C_{22}H_{31}N_6O_4$ $[M+H]^+$: 443.24068; found: 443.23941. $[\alpha]_D$: −20.5° (5.4 mg/ml, MeOH).

Compound 6h. Following the general procedure for CuAAC, starting from compound **4** (200 mg, 0.70 mmol) and 1-boc-4-ethynylpiperidine **5h** (293 mg, 1.40 mmol), and using DCM/MeOH (96/4) as eluent for flash chromatography purification, compound **6h** was obtained as a colorless oil (336 mg, 97%). ^{1}H NMR (500 MHz, $CDCl_3$) δ 7.37 – 7.27 (m, 5H, $H_{18, 19, 20}$), 4.96 (d, J = 11.5 Hz, 1H, H_{16}), 4.82 (d, J = 11.5 Hz, 1H, H_{16}), 4.49 (bs, 2H, H_7), 4.10 (bs, 2H, H_{12}), 3.76 (bs, 1H, H_1), 3.32 (s, 1H, H_4), 2.88 (bs, 5H, $H_{5, 10, 12}$), 2.01 – 1.98 (m, 3H, $H_{3, 11}$), 1.94 – 1.87 (m, 1H, H_2), 1.68 – 1.62 (m, 1H, H_3), 1.57 – 1.51 (m, 3H, $H_{2, 11}$), 1.42 (s, 9H, H_{15})**H*$_8$ not visible on the ^{1}H NMR spectrum*. ^{13}C NMR (125 MHz, $CDCl_3$) δ 169.2 (C_6), 154.7 (C_{13}), 135.7 (C_{17}), 129.1 (C_{19}), 128.7 (C_{20}), 128.5 (C_{18}), 79.4 (C_{14}), 78.1 (C_{16}), 58.3 (C_4), 56.5 (C_1), 52.1 (C_7), 43.6 (2C, C_5 and C_{12}), 33.6 (C_{10}), 31.4 (C_{11}), 28.4 (C_{15}), 20.4 (C_2), 19.6 (C_3) **C*$_8$ *and C*$_9$ *not visible on the ^{13}C NMR spectrum.* HRMS calculated for $C_{26}H_{37}N_6O_4$ $[M+H]^+$: 497.28763; found: 497.28723. $[\alpha]_D$: −6.3° (6.3 mg/ml, MeOH).

Compound 6i. Following the general procedure for CuAAC, starting from compound **4** (90 mg, 0.31 mmol) and **5i** (181 mg, 0.63 mmol) and using DCM/MeOH (96/4) as eluent for flash chromatography purification, compound **6i** was obtained as a pale yellow solid (163 mg, 91%). ^{1}H NMR (500 MHz, $CDCl_3$) δ 8.35 (bd, J = 12.5 Hz, 1H, NH), 7.85 (s, 1H, H_8), 7.68 (d, J = 8.1 Hz, 2H, H_{11}), 7.57 (d, J = 8.2 Hz, 2H, H_{12}), 7.40 – 7.31 (m, 5H, $H_{22, 23, 24}$), 5.31 (bs, 1H, NH), 5.00 (d, J = 11.5 Hz, 1H, H_{20}), 4.86 (d, J = 11.5 Hz, 1H, H_{20}), 4.56 (dd, J = 14.2, 8.0 Hz, 1H, H_7), 4.50 (dd, J = 14.3, 6.9 Hz, 1H, H_7), 3.86 – 3.81 (m, 1H, H_1), 3.49 – 3.45 (m, 2H, H_{16}), 3.35 (bs, 1H, H_4), 2.94 (s, 2H, H_5), 2.60 (t, J = 5.5 Hz, 2H, H_{15}), 2.07 – 2.02 (m, 1H, H_3), 2.00 – 1.92 (m, 1H, H_2), 1.71 – 1.64 (m, 1H, H_3), 1.60 – 1.54 (m, 1H, H_2), 1.42 (s, 9H, H_{19}). ^{13}C NMR (125 MHz, $CDCl_3$) δ 170.1 (C_{14}), 169.5 (C_6), 156.5 (C_{17}), 147.8 (C_9), 138.2 (C_{10}), 135.7 (C_{21}), 129.3 (C_{23}), 128.9 (C_{24}), 128.7 (C_{22}), 126.4 (2C, C_{11} and C_{13}), 120.2 (C_{12}), 119.9 (C_8), 79.7 (C_{18}), 78.3 (C_{20}), 58.4 (C_4), 56.7 (C_1), 51.9 (C_7), 43.9 (C_5), 37.6 (C_{15}), 36.6 (C_{16}), 28.5 (C_{19}), 20.3 (C_2), 19.8 (C_3). HRMS calculated for $C_{30}H_{38}N_7O_5$ $[M+H]^+$: 576.29344; found: 576.29582. $[\alpha]_D$: −13.5° (4.0 mg/ml, MeOH).

Compound 6j. Following the general procedure for CuAAC, starting from compound **4** (200 mg, 0.70 mmol) and 4-pentynoic acid **5j** (137 mg, 1.40 mmol), and using DCM/MeOH (9/1) as eluent for flash chromatography purification, compound **6j** was obtained as a pale yellow solid (202 mg, 75%). ^{1}H NMR (500 MHz, $CDCl_3$) δ 7.57 (s, 1H, H_8), 7.41 – 7.33 (m, 5H, $H_{15, 16, 17}$), 5.01 (d, J = 11.5 Hz, 1H, H_{13}), 4.87 (d, J = 11.5 Hz, 1H, H_{13}), 4.53 - 4.44 (m, 2H, H_7), 3.82 – 3.77 (m, 1H, H_1), 3.35 (bd, J = 2.8 Hz, 1H, H_4), 3.03 (t, J = 6.4 Hz, 2H, H_{10}), 2.95 – 2.88 (m, 2H, H_5), 2.75 (t, J = 6.2 Hz, 2H, H_{11}), 2.07 – 2.01 (m, 1H, H_3), 1.94 (dq, J = 15.1, 7.5 Hz, 1H, H_2), 1.69 – 1.63 (m, 1H, H_3), 1.58 – 1.52 (m, 1H, H_2). ^{13}C NMR (125 MHz, $CDCl_3$) δ 175.8 (C_{12}), 169.5 (C_6), 146.8 (C_9), 135.8 (C_{14}), 129.4 (C_{16}), 128.9 (C_{17}), 128.7 (C_{15}), 122.0 (C_8), 78.4 (C_{13}), 58.4 (C_4), 56.7 (C_1), 51.9 (C_7), 43.9 (C_5), 33.5 (C_{11}), 21.0 (C_{10}), 20.3 (C_2), 19.8 (C_3). HRMS calculated for $C_{19}H_{24}N_5O_4$ $[M+H]^+$: 386.18283; found: 386.18228. $[\alpha]_D$: −23.8° (7.9 mg/ml, MeOH).

Compound 7a. Following the general procedure for the introduction of sodium sulphite, compound **7a** was obtained as a white powder (18 mg, 21%) starting from compound **6a** (83 mg, 0.21 mmol). ^{1}H NMR (500 MHz, D_2O) δ 8.81 (bs, 1H, H_{14}), 8.50 (bd, J = 4.8 Hz, 1H, H_{13}), 8.44 (s, 1H, H_8), 8.12 (bd, J = 8.0

Hz, 1H, H_{11}), 7.52 (dd, *J* = 7.9, 5.0 Hz, 1H, H_{12}), 4.97 (dd, *J* = 14.8, 10.6 Hz, 1H, H_7), 4.71 (dd, *J* = 14.8, 5.6 Hz, 1H, H_7), 4.31 – 4.29 (m, 1H, H_4), 4.01 – 3.96 (m, 1H, H_1), 3.56 (d, *J* = 12.3 Hz, 1H, H_5), 3.24 (bd, *J* = 12.2 Hz, 1H, H_5), 2.18 – 2.12 (m, 1H, H_3), 2.09 – 1.99 (m, 2H, $H_{2,3}$), 1.81 – 1.74 (m, 1H, H_2). ^{13}C NMR (125 MHz, D_2O) δ 170.2 (C_6), 148.3 (C_{13}), 145.5 (C_{14}), 144.3 (C_9), 134.1 (C_{11}), 126.1 (C_{10}), 124.5 (C_{12}), 122.8 (C_8), 60.1 (C_4), 57.9 (C_1), 50.8 (C_7), 43.6 (C_5), 19.8 (C_2), 18.8 (C_3). HRMS calculated for $C_{14}H_{14}N_6O_5S$ [M-H]$^-$: 379.08246; found: 379.08392. [α]$_D$: –44.6° (9.1 mg/ml, MeOH). HPLC purity = 98.7%; rt = 9.4 min (CH_3CN/H_2O 0:100 to 100:0 over 15 min).

Compound 7b. Following the general procedure for the introduction of sodium sulphite, compound **7b** was obtained as a white powder (44 mg, 19%) starting from compound **6b** (226 mg, 0.58 mmol). ^{1}H NMR (500 MHz, D_2O) δ 8.28 (s, 1H, H_8), 7.77 (d, *J* = 7.3 Hz, 2H, H_{11}), 7.53 (t, *J* = 7.3 Hz, 2H, H_{12}), 7.46 (d, *J* = 7.3 Hz, 1H, H_{13}), 4.86 (dd, *J* = 14.8, 10.2 Hz, 1H, H_7), 4.62 (dd, *J* = 14.7, 5.7 Hz, 1H, H_7), 4.30 – 4.28 (m, 1H, H_4), 3.95 – 3.91 (m, 1H, H_1), 3.50 (d, *J* = 12.3 Hz, 1H, H_5), 3.22 (bd, J = 12.2 Hz, 1H, H_5), 2.15 – 2.09 (m, 1H, H_3), 2.04 – 1.95 (m, 2H, $H_{2,3}$), 1.77 – 1.68 (m, 1H, H_2). ^{13}C NMR (125 MHz, D_2O) δ 170.1 (C_6), 147.6 (C_9), 129.4 (C_{10}), 129.2 (C_{12}), 128.8 (C_{13}), 125.6 (C_{11}), 122.3 (C_8), 60.1 (C_4), 57.8 (C_1), 50.8 (C_7), 43.6 (C_5), 19.7 (C_2), 18.8 (C_3). HRMS calculated for $C_{15}H_{16}N_5O_5S$ [M-H]$^-$: 378.08721; found: 378.08804. [α]$_D$: –36.7° (10.7 mg/ml, H_2O). HPLC purity = 98.1%; rt = 10.4 min (CH_3CN/H_2O 0:100 to 100:0 over 15 min).

Compound 7c. Following the general procedure for the introduction of sodium sulphite, compound **7c** was obtained as a white powder (12 mg, 14%) starting from compound **6c** (82 mg, 0.21 mmol). ^{1}H NMR (500 MHz, D_2O) δ 8.15 (s, 1H, H_8), 4.95 (dd, *J* = 14.7, 10.0 Hz, 1H, H_7), 4.72 (dd, *J* = 14.7, 5.9 Hz, 1H, H_7), 4.29 – 4.28 (m, 1H, H_4), 3.97 – 3.92 (m, 1H, H_1), 3.50 (d, *J* = 12.3 Hz, 1H, H_5), 3.23 – 3.20 (m, 1H, H_5), 2.17 – 2.09 (m, 1H, H_3), 2.05 – 1.96 (m, 2H, $H_{2,3}$), 1.76 – 1.69 (m, 1H, H_2), 0.35 (s, 9H, H_{10}). ^{13}C NMR (125 MHz, D_2O) δ 170.2 (C_6), 147.7 (C_9), 131.4 (C_8), 60.0 (C_4), 57.9 (C_1), 50.1 (C_7), 43.6 (C_5), 19.6 (C_2), 18.8 (C_3), -2.3 (C_{10}). HRMS calculated for $C_{12}H_{19}N_5O_5SSi$ [M-H]$^-$: 374.09544; found: 374.09427. [α]$_D$: –52.0° (2.0 mg/ml, MeOH). HPLC purity = 96.1%; rt = 10.6 min (CH_3CN/H_2O 0:100 to 100:0 over 15 min).

Compound 7d. Following the general procedure for the introduction of sodium sulphite, compound **7d** was obtained as a colorless foam (28 mg, 13%) starting from compound **6d** (210 mg, 0.59 mmol). ^{1}H NMR (500 MHz, D_2O) δ 8.18 (s, 1H, H_8), 4.96 (dd, *J* = 14.8, 10.3 Hz, 1H, H_7), 4.73 (dd, *J* = 14.8, 5.7 Hz, 1H, H_7), 4.68 (s, 2H, H_{10}), 4.32 – 4.30 (m, 1H, H_4), 4.00 – 3.95 (m, 1H, H_1), 3.55 (d, *J* = 12.3 Hz, 1H, H_5), 3.45 (s, 3H, H_{11}), 3.25 (bd, *J* = 12.3 Hz, 1H, H_5), 2.19 – 2.13 (m, 1H, H_3), 2.08 – 1.99 (m, 2H, $H_{2,3}$), 1.80 – 1.76 (m, 1H, H_2). ^{13}C NMR (125 MHz, D_2O) δ 170.1 (C_6), 144.0 (C_9), 125.4 (C_8), 64.4 (C_{10}), 60.1 (C_4), 57.9 (C_1), 57.5 (C_{11}), 50.7 (C_7), 43.6 (C_5), 19.7 (C_2), 18.8 (C_3). HRMS calculated for $C_{11}H_{16}N_5O_6S$ [M-H]$^-$: 346.08213; found: 346.08185. HPLC purity = 98.3%; rt = 13.5 min (CH_3CN + 0.1% TFA / H_2O + 0.1% TFA 0:100 to 100:0 over 30 min).

Compound 7e. Starting from compound **6e** (173 mg, 0.47 mmol) and following the general procedure for the introduction of sodium sulphite, product **7e** was obtained as a white powder (32 mg, 18%) in the form of a mixture of two isomers. ^{1}H NMR (500 MHz, D_2O) δ 8.50 (s, 0,5H, H_8), 8.38 (s, 0,5H, $H_{8'}$), 5.03 – 4.96 (m, 1H, $H_{7,7'}$), 4.77 – 4.72 (m, 1H, $H_{7,7'}$), 4.71 (s, 1H, H_{10}), 4.52 (s, 1H, $H_{10'}$), 4.30 (bs, 1H, $H_{4,4'}$), 3.99 – 3.93 (m, 1H, $H_{1,1'}$), 3.57 (dd, *J* = 12.3, 7.8 Hz, 1H, $H_{5,5'}$), 3.23 (bd, *J* = 12.3 Hz, 1H, $H_{5,5'}$), 3.19 (s, 3H, H_{11}), 2.94 (s, 3H, $H_{11'}$), 2.15 – 2.10 (m, 1H, $H_{3,3'}$), 2.09 – 1.98 (m, 2H, $H_{2,3,2',3'}$), 1.83 – 1.77 (m, 1H, $H_{2,2'}$). ^{13}C NMR (125 MHz, D_2O) δ 170.1 (2C, C_6 and $C_{6'}$), 136.7 ($C_{9'}$), 135.6 (C_9), 129.1 (C_8), 127.7 ($C_{8'}$), 60.1 (C_{10}), 59.8 (2C, C_4 and $C_{4'}$), 58.1 ($C_{1 \text{ or } 1'}$), 58.0 ($C_{1 \text{ or } 1'}$), 52.6 (C_{11}), 51.1 ($C_{10'}$), 51.0 ($C_{7 \text{ or } 7'}$), 50.9 ($C_{7 \text{ or } 7'}$), 43.4 (2C, C_5 and $C_{5'}$), 42.2 ($C_{11'}$), 19.9 ($C_{2 \text{ or } 2'}$), 19.8 ($C_{2 \text{ or } 2'}$), 18.8 (2C, C_3 and $C_{3'}$). HRMS calculated for $C_{12}H_{19}N_6O_5S$ [M-H]$^-$: 359.11376; found: 359.11426. [α]$_D$: –27.7° (11.0 mg/ml, H_2O). HPLC purity = 98.1%; rt = 6.8 min (CH_3CN/H_2O 0:100 to 100:0 over 15 min).

Compound 7f. Following the general procedure for the introduction of sodium sulphite, compound **7f** was obtained as a white powder (6 mg, 8%) starting from compound **6f** (74 mg, 0.18 mmol). ^{1}H NMR (500 MHz, D_2O) δ 8.12 (s, 1H, H_8), 4.95 (dd, *J* = 14.7, 10.3 Hz, 1H, H_7), 4.71 (dd, *J* = 14.7, 5.7 Hz, 1H, H_7), 4.31 – 4.30 (m, 1H, H_4), 3.99 – 3.94 (m, 1H, H_1), 3.82 – 3.79 (m, 6H, $H_{10,12}$), 3.54 (d, *J* = 12.3 Hz, 1H, H_5), 3.24 (bd, *J* = 12.1 Hz, 1H, H_5), 2.67 (bs, 4H, H_{11}), 2.16 – 2.12 (m, 1H, H_3), 2.08 – 1.98 (m, 2H, $H_{2,3}$), 1.80 – 1.75 (m, 1H, H_2). ^{13}C NMR (125 MHz, D_2O) δ 170.2 (C_6), 142.0 (C_9), 125.8 (C_8), 66.0 (C_{12}), 60.1 (C_4), 57.9 (C_1), 51.9 (C_{11}), 51.6 (C_{10}), 50.7 (C_7), 43.6 (C_5), 19.7 (C_2), 18.8 (C_3). HRMS calculated for $C_{14}H_{21}N_6O_6S$ [M-H]-: 401.12433; found: 401.12557. [α]$_D$: –37.2° (1.8 mg/ml, MeOH). HPLC purity = 95.1%; rt = 6.0 min (CH_3CN/H_2O 0:100 to 100:0 over 15 min).

Compound 7g. Following the general procedure for the introduction of sodium sulphite, compound **7g** was obtained as a white solid (88 mg, 30%) starting from compound **6g** (283 mg, 0.64 mmol). ^{1}H NMR (500 MHz, D_2O) δ 8.01 (s, 1H, H_8), 4.92 (dd, *J* = 14.8, 10.3 Hz, 1H, H_7), 4.69 (dd, *J* = 14.8, 5.7 Hz, 1H, H_7), 4.39 (s, 2H, H_{10}), 4.31 – 4.29 (m, 1H, H_4), 3.97 – 3.92 (m, 1H, H_1), 3.53 (d, *J* = 12.3 Hz, 1H, H_5), 3.23 (bd, *J* = 12.2 Hz, 1H, H_5), 2.16 – 2.11 (m, 1H, H_3), 2.07 – 1.97 (m, 2H, $H_{2,3}$), 1.78 – 1.74 (m, 1H, H_2), 1.47 (s, 9H, H_{13}). ^{13}C NMR (125 MHz, D_2O) δ 170.1 (C_6), 158.0 (C_{11}), 146.0 (C_9), 123.8 (C_8), 81.4 (C_{12}), 60.1 (C_4), 57.9 (C_1), 50.7 (C_7), 43.6 (C_5), 35.4 (C_{10}), 27.6 (C_{13}), 19.7 (C_2), 18.8 (C_3). HRMS calculated for $C_{15}H_{23}N_6O_7S$ [M-H]$^-$: 431.13489; found: 431.13669. [α]$_D$: –35.6° (13.6 mg/ml, H_2O). HPLC purity = 96.9%; rt = 10.2 min (CH_3CN/H_2O 0:100 to 100:0 over 15 min).

Compound 7h. Following the general procedure for the introduction of sodium sulphite, compound **7h** was obtained as a white powder (184 mg, 53%) starting from compound **6h** (336 mg, 0.68 mmol). ^{1}H NMR (500 MHz, D_2O) δ 7.94 (s, 1H, H_8), 4.90 (dd, *J* = 14.7, 10.2 Hz, 1H, H_7), 4.67 (dd, *J* = 14.7, 5.8 Hz, 1H, H_7), 4.31 – 4.29 (m, 1H, H_4), 4.13 (bd, *J* = 12.7 Hz, 2H, H_{12}), 3.97 – 3.92 (m, 1H, H_1), 3.51 (d, *J* = 12.3 Hz, 1H, H_5), 3.22 (bd, *J* = 12.3 Hz, 1H, H_5), 3.08 – 3.01 (m, 3H, $H_{10,12}$), 2.17 – 2.11 (m, 1H, H_3), 2.07 – 1.98 (m, 4H, $H_{2,3,11}$), 1.77 – 1.71 (m, 1H, H_2), 1.66 – 1.59 (m, 2H, H_{11}), 1.51 (s, 9H, H_{15}). ^{13}C NMR (125 MHz, D_2O) δ 170.1 (C_6), 156.6 (C_{13}), 152.0 (C_9), 122.4 (C_8), 81.6 (C_{14}), 60.1 (C_4), 57.9 (C_1), 50.6 (C_7), 43.6 (2C, C_5 and C_{12}), 32.5 (C_{10}), 31.0 (C_{11}), 27.7 (C_{15}), 19.7 (C_2), 18.8 (C_3). HRMS calculated for $C_{19}H_{30}N_6O_7S$ [M+H]$^+$: 487.19749; found: 487.19849. [α]$_D$: –21.1° (11.8 mg/ml, H_2O). HPLC purity = 95.1%; rt = 11.8 min (CH_3CN/H_2O 0:100 to 100:0 over 15 min).

Compound 7i. Following the general procedure for the introduction of sodium sulphite, compound **7i** was obtained as a white powder (37 mg, 23%) starting from compound **6i** (159

mg, 0.28 mmol). ^{1}H NMR (500 MHz, D_2O) δ 8.26 (s, 1H, H_8), 7.71 (d, *J* = 8.4 Hz, 2H, H_{11}), 7.52 (d, *J* = 8.2 Hz, 2H, H_{12}), 4.85 (dd, *J* = 14.8, 10.2 Hz, 1H, H_7), 4.61 (dd, *J* = 14.8, 5.8 Hz, 1H, H_7), 4.29 – 4.27 (m, 1H, H_4), 3.94 – 3.90 (m, 1H, H_1), 3.49 (d, *J* = 12.2 Hz, 1H, H_5), 3.46 (t, *J* = 6.1 Hz, 2H, H_{16}), 3.21 (d, *J* = 12.1 Hz, 1H, H_5), 2.59 (t, *J* = 5.9 Hz, 2H, H_{15}), 2.15 – 2.09 (m, 1H, H_3), 2.03 – 1.94 (m, 2H, $H_{2,3}$), 1.74 – 1.67 (m, 1H, H_2), 1.39 (s, 9H, H_{19}). ^{13}C NMR (125 MHz, D_2O) δ 172.9 (C_{14}), 170.1 (C_6), 158.0 (C_{17}), 147.2 (C_9), 137.3 (C_{10}), 126.3 ($C_{11 \text{ or } 13}$), 126.2 ($C_{11 \text{ or } 13}$), 122.1 (C_8), 121.8 (C_{12}), 81.0 (C_{18}), 60.1 (C_4), 57.8 (C_1), 50.8 (C_7), 43.6 (C_5), 37.2 (C_{15}), 36.8 (C_{16}), 27.6 (C_{19}), 19.7 (C_2), 18.8 (C_3). HRMS calculated for $C_{23}H_{29}N_7O_8S$ [M-H]$^-$: 564.18766; found: 564.18766. [α]$_D$: −12.2° (3.0 mg/ml, MeOH). HPLC purity = 99.1%; rt = 11.4 min (CH_3CN/H_2O 0:100 to 100:0 over 15 min).

Compound 7j. Following the general procedure for the introduction of sodium sulphite, compound **7j** was obtained as a colorless foam (34 mg, 17%) starting from compound **6j** (194 mg, 0.50 mmol). ^{1}H NMR ^{1}H NMR (500 MHz, D_2O) δ 7.87 (s, 1H, H_8), 4.89 (dd, *J* = 14.8, 10.1 Hz, 2H, H_7), 4.66 (dd, *J* = 14.8, 6.0 Hz, 2H, H_7), 4.29 – 4.28 (m, 1H, H_4), 3.97 – 3.91 (m, 1H, H_1), 3.51 (d, *J* = 12.4 Hz, 1H, H_5), 3.21 (bd, *J* = 12.3 Hz, 1H, H_5), 2.99 (t, *J* = 7.6 Hz, 2H, H_{10}), 2.57 (t, *J* = 7.6 Hz, 2H, H_{11}), 2.15 – 2.09 (m, 1H, H_3), 2.04 – 1.96 (m, 2H, $H_{2,3}$), 1.76 – 1.69 (m, 1H, H_2). ^{13}C NMR (125 MHz, D_2O) δ 181.7 (C_{12}), 170.1 (C_6), 148.0 (C_9), 123.3 (C_8), 60.0 (C_4), 57.8 (C_1), 50.5 (C_7), 43.7 (C_5), 36.7 (C_{11}), 21.8 (C_{10}), 19.6 (C_2), 18.8 (C_3). HRMS calculated for $C_{12}H_{16}N_5O_7S$ [M-H]$^-$: 374.07704; found: 374.07651. [α]$_D$: −17.2° (16.4 mg/ml, H_2O). HPLC purity = 96,0%; rt = 13.5 min (CH_3CN + 0.1% TFA / H_2O + 0.1% TFA 0:100 to 100:0 over 30 min).

Compound 8g. Following the general procedure for the deprotection of Boc, compound **8g** was obtained as a white powder (7.4 mg, 36%) starting from compound **7g** (21 mg, 0.05 mmol). ^{1}H NMR (500 MHz, D_2O) δ 8.26 (s, 1H, H_8), 4.99 (dd, *J* = 14.8, 10.9 Hz, 1H, H_7), 4.72 (dd, *J* = 14.8, 5.2 Hz, 1H, H_7), 4.40 (s, 2H, H_{10}), 4.32 – 4.30 (m, 1H, H_4), 3.99 – 3.94 (m, 1H, H_1), 3.57 (d, *J* = 12.3 Hz, 1H, H_5), 3.24 (bd, *J* = 12.3 Hz, 1H, H_5), 2.17 – 2.12 (m, 1H, H_3), 2.10 – 1.99 (m, 2H, $H_{2,3}$), 1.82 – 1.78 (m, 1H, H_2). ^{13}C NMR (125 MHz, D_2O) δ 170.1 (C_6), 140.0 (C_9), 125.5 (C_8), 60.1 (C_4), 58.0 (C_1), 50.8 (C_7), 43.5 (C_5), 34.1 (C_{10}), 19.8 (C_2), 18.8 (C_3). HRMS calculated for $C_{10}H_{15}N_6O_5S$ [M-H]$^-$: 331.08246; found: 331.08277. [α]$_D$: −40.2° (2.5 mg/ml, H_2O). HPLC purity = 97.7%; rt = 4.0 min (CH_3CN/H_2O 0:100 to 100:0 over 15 min).

Compound 8h. Following the general procedure for the deprotection of Boc, compound **8h** was obtained as a white powder (20 mg, 34%) starting from compound **7h** (59 mg, 0.12 mmol). ^{1}H NMR (500 MHz, D_2O) δ 8.00 (s, 1H, H_8), 4.91 (dd, *J* = 14.8, 10.6 Hz, 1H, H_7), 4.66 (dd, *J* = 14.8, 5.5 Hz, 1H, H_7), 4.29 – 4.27 (m, 1H, H_4), 3.96 – 3.91 (m, 1H, H_1), 3.57 – 3.51 (m, 3H, $H_{5,12}$), 3.25 – 3.18 (m, 4H, $H_{5,10,12}$), 2.33 – 2.29 (m, 3H, 2H, H_{11}), 2.16 – 2.09 (m, 1H, H_3), 2.06 – 1.93 (m, 4H, $H_{2,3,11}$), 1.77 – 1.71 (m, 1H, H_2). ^{13}C NMR (125 MHz, D_2O) δ 170.1 (C_6), 150.3 (C_9), 122.6 (C_8), 60.1 (C_4), 57.9 (C_1), 50.7 (C_7), 43.6 (2C, C_5 and C_{12}), 30.28 (C_{10}), 27.8 (C_{11}), 19.7 (C_2), 18.82 (C_3). HRMS calculated for $C_{14}H_{21}N_6O_5S$ [M-H]$^-$: 385.12941; found: 385.13052. [α]$_D$: −37.2° (13.7 mg/ml, H_2O). HPLC purity = 97.6%; rt = 9.6 min (CH_3CN/H_2O 0:100 to 100:0 over 15 min).

Compound 8i. Following the general procedure for the deprotection of Boc, compound **8i** was obtained as a white solid (2.4 mg, 17%) starting from compound **7i** (14 mg, 0.02 mmol). ^{1}H NMR (500 MHz, $(CD_3)_2SO$) δ 10.21 (s, 1H, NH), 8.49 (s, 1H, H_8), 7.80 (d, *J* = 8.7 Hz, 2H, H_{11}), 7.68 (d, *J* = 8.7 Hz, 2H, H_{12}), 4.79 (dd, *J* = 14.3, 9.8 Hz, 1H, H_7), 4.59 (dd, *J* = 14.4, 6.1 Hz, 1H, H_7), 4.04 – 4.02 (m, 1H, H_4), 3.68 – 3.63 (m, 1H, H_1), 3.40 (d, *J* = 11.9 Hz, 1H, H_5), 3.11 (t, *J* = 6.5 Hz, 2H, H_{16}), 2.91 (bd, *J* = 11.9 Hz, 1H, H_5), 2.71 (t, *J* = 6.5 Hz, 2H, H_{15}), 1.87 – 1.75 (m, 3H, $H_{2,3}$), 1.56 – 1.50 (m, 1H, H_2). ^{13}C NMR (125 MHz, $(CD_3)_2SO$) δ 168.4 (C_{14}), 167.3 (C_6), 146.1 (C_9), 138.3 (C_{10}), 126.0 (C_{13}), 125.7 (C_{11}), 121.2 (C_8), 119.4 (C_{12}), 58.1 (C_4), 56.9 (C_1), 50.5 (C_7), 43.3 (C_5), 34.8 (C_{16}), 33.0 (C_{15}), 19.8 (C_2), 19.3 (C_3). HRMS calculated for $C_{18}H_{22}N_7O_6S$ [M-H]$^-$: 464.13523; found: 464.13516. HPLC purity = 98.5%; rt = 10.5 min (CH_3CN/H_2O 0:100 to 100:0 over 15 min).

Compound 2. Ethyl chloroformate (115 µl, 1.20 mmol) was added dropwise at -10°C to a solution of compound **1** (300 mg, 1.09 mmol) and N-methylmorpholine (358 µl, 3.26 mmol) in THF (5 ml). The solution was stirred at -10°C for 1 h then at 5°C overnight. The reaction mixture was cooled again to -10°C and $NaBH_4$ (124 mg, 3.26 mmol) was added gradually. The solution was then stirred for 1 h 30 min at -10°C. Water (5 ml) and ethyl acetate (5 ml) were slowly added and the heterogeneous mixture was stirred for 30 min at room temperature. The phases were separated, and the aqueous layer was extracted with ethyl acetate. The combined organic layers were washed with brine, dried over $MgSO_4$, and concentrated under reduced pressure. Purification by flash chromatography using DCM/MeOH (96/4) as the eluent gave compound **2** as a colorless oil (88 mg, 31%). ^{1}H NMR (500 MHz, $CDCl_3$) δ 7.40 – 7.29 (m, 5H, $H_{10,11,12}$), 5.00 (d, *J* = 11.4 Hz, 1H, H_8), 4.85 (d, *J* = 11.4 Hz, 1H, H_8), 3.69 (dd, *J* = 11.3, 9.4 Hz, 1H, H_7), 3.57 (dd, *J* = 11.4, 5.5 Hz, 1H, H_7), 3.52 – 3.47 (m, 1H, H_1), 3.33 – 3.31 (m, 1H, H_4), 2.99 (d, *J* = 11.7 Hz, 1H, H_5), 2.87 (bd, *J* = 11.6 Hz, 1H, H_5), 1.99 – 1.93 (m, 1H, H_3), 1.93 – 1.86 (m, 1H, H_2), 1.57 – 1.51 (m, 1H, H_3), 1.41 – 1.35 (m, 1H, H_2). ^{13}C NMR (125 MHz, $CDCl_3$) δ 170.1 (C_6), 136.1 (C_9), 129.4 (C_{11}), 128.8 (C_{12}), 128.7 (C_{10}), 78.4 (C_8), 62.6 (C_7), 58.8 (C_1), 58.6 (C_4), 43.5 (C_5), 20.1 (C_3), 19.4 (C_2). HRMS calculated for $C_{14}H_{19}N_2O_3$ [M+H]$^+$: 263.13957; found: 263.13852. [α]$_D$: −54.5° (4.0 mg/ml, MeOH).

Compound 9a and 9b. N,N-Diisopropylethylamine (598 µl, 3.43 mmol), DMAP (14 mg, 0.11 mmol) and MsCl (133 µl, 1.72 mmol) were added at 0°C to a solution of **2** (300 mg, 1.14 mmol) in DCM (25 ml). The reaction mixture was stirred at 0°C for 1 h. DCM was then added and the organic layer was washed with brine, dried over $MgSO_4$ and concentrated under vacuum to afford compound **3** which was used in the next step without further purification. A solution of crude product **3** (1.14 mmol) in acetonitrile (18 ml) was added dropwise to a solution of 1H-1,2,3-triazole (133 µl, 2.29 mmol) and tBuOK (257 mg, 2.29 mmol) in acetonitrile (24 ml). The reaction mixture was stirred at 90°C for 15 h. DCM was then added and the organic layer was washed with H_2O and brine, dried over $MgSO_4$ and concentrated under vacuum. Purification by flash chromatography using cyclohexane/ethyl acetate (9/1) as the eluent gave compounds **9a** (164 mg, 44% over 2 steps) and **9b** (136 mg, 37% over 2 steps) as orange solids. **9a:** ^{1}H NMR (500 MHz, $CDCl_3$) δ 7.55 (s, 2H, H_8), 7.38 – 7.27 (m, 5H, $H_{11,12,13}$), 4.98 (d, *J* = 11.5 Hz, 1H, H_9), 4.84 (d, *J* = 11.5 Hz, 1H, H_9), 4.66 (dd, *J* = 13.8, 7.7 Hz, 1H, H_7), 4.52 (dd, *J* = 13.8, 7.7 Hz, 1H, H_7), 4.03 – 3.98 (m, 1H, H_1), 3.32 (q, *J* = 3.0 Hz, 1H, H_4), 2.99 (d, *J* = 11.9 Hz, 1H, H_5), 2.90 (dt, *J* = 11.9, 3.0 Hz, 1H, H_5), 2.01 – 1.95 (m, 1H, H_3), 1.93 – 1.86 (m, 1H, H_2), 1.63 – 1.57 (m, 1H, H_3), 1.46 – 1.40 (m, 1H, H_2).^{13}C NMR (125 MHz, $CDCl_3$)

δ 169.2 (C_6), 135.8 (C_{10}), 134.5 (C_8), 129.1 (C_{12}), 128.6 (C_{13}), 128.4 (C_{11}), 78.1 (C_9), 58.2 (C_4), 56.6 (C_1), 55.9 (C_7), 44.3 (C_5), 19.9 (C_2), 19.8 (C_3). HRMS calculated for $C_{16}H_{20}N_5O_2$ $[M+H]^+$: 314.16170 ; found: 314.16104. $[\alpha]_D$: – 32.3° (6.0 mg/ml, MeOH). **9b:** ^{1}H NMR (500 MHz, $CDCl_3$) δ 7.72 (d, *J* = 0.8 Hz, 1H, H_8), 7.66 (d, *J* = 0.8 Hz, 1H, H_9), 7.39 – 7.29 (m, 5H, $H_{12, 13, 14}$), 4.98 (d, *J* = 11.5 Hz, 1H, H_{10}), 4.84 (d, *J* = 11.5 Hz, 1H, H_{10}), 4.56 (dd, *J* = 14.2, 8.0 Hz, 1H, H_7), 4.51 (dd, *J* = 14.2, 6.9 Hz, 1H, H_7), 3.81 – 3.76 (m, 1H, H_1), 3.36 – 3.34 (m, 1H, H_4), 2.90 (bs, 2H, H_5), 2.05 – 1.99 (m, 1H, H_3), 1.96 – 1.89 (m, 1H, H_2), 1.69 – 1.62 (m, 1H, H_3), 1.57 – 1.51 (m, 1H, H_2). ^{13}C NMR (125 MHz, $CDCl_3$) δ 169.3 (C_6), 135.7 (C_{11}), 134.1 (C_9), 129.2 (C_{13}), 128.8 (C_{14}), 128.6 (C_{12}), 124.0 (C_8), 78.2 (C_{10}), 58.3 (C_4), 56.7 (C_1), 51.7 (C_7), 43.7 (C_5), 20.3 (C_2), 19.7 (C_3). HRMS calculated for $C_{16}H_{20}N_5O_2$ $[M+H]^+$: 314.16170; found: 314.16113. $[\alpha]_D$: –32.9° (3.4 mg/ml, MeOH).

Compound 10a. Following the general procedure for the introduction of sodium sulphite, compound **10a** was obtained as a yellow solid (44 mg, 27%) starting from compound **9a** (158 mg, 0.51 mmol). ^{1}H NMR ^{1}H NMR (500 MHz, D_2O) δ 7.89 (s, 2H, H_8), 5.04 (dd, *J* = 14.7, 10.4 Hz, 1H, H_7), 4.77 (dd, *J* = 14.7, 5.8 Hz, 1H, H_7), 4.33 – 4.31 (m, 1H, H_4), 4.10 - 4.05 (m, 1H, H_1), 3.58 (d, *J* = 12.3 Hz, 1H, H_5), 3.22 (bd, *J* = 12.3 Hz, 1H, H_5), 2.19 – 2.12 (m, 1H, H_3), 2.08 – 1.99 (m, 2H, $H_{2, 3}$), 1.81 – 1.73 (m, 1H, H_2). ^{13}C NMR (125 MHz, D_2O) δ 169.9 (C_6), 135.1 (C_8), 60.0 (C_4), 57.8 (C_1), 54.6 (C_7), 43.9 (C_5), 19.5 (C_2), 18.9 (C_3). HRMS calculated for $C_9H_{12}N_5O_5S$ $[M-H]^-$: 302.05591; found: 302.05685. $[\alpha]_D$: –37.4° (18.0 mg/ml, H_2O). HPLC purity = 97.0%; rt = 2.8 min (CH_3CN / H_2O 0:100 to 100:0 over 30 min).

*Compound 10b***.** Following the general procedure for the introduction of sodium sulphite, compound **10b** was obtained as a white foam (14 mg, 8%) starting from compound **9b** (132 mg, 0.42 mmol). ^{1}H NMR ^{1}H NMR (500 MHz, D_2O) δ 8.13 (s, 1H, H_8), 7.88 (s, 1H, H_9), 5.00 (dd, *J* = 14.8, 10.5 Hz, 1H, H_7), 4.74 (dd, *J* = 14.8, 5.6 Hz, 1H, H_7), 4.32 – 4.30 (m, 1H, H_4), 4.01 – 3.96 (m, 1H, H_1), 3.57 (d, *J* = 12.3 Hz, 1H, H_5), 3.24 (bd, *J* = 12.3 Hz, 1H, H_5), 2.19 – 2.12 (m, 1H, H_3), 2.09 – 1.99 (m, 2H, $H_{2, 3}$), 1.82 – 1.74 (m, 1H, H_2). ^{13}C NMR (125 MHz, D_2O) δ 170.1 (C_6), 134.2 (C_9), 125.9 (C_8), 60.0 (C_4), 58.0 (C_1), 50.4 (C_7), 43.6 (C_5), 19.7 (C_2), 18.8 (C_3). HRMS calculated for $C_9H_{12}N_5O_5S$ $[M-H]^-$: 302.05591; found: 302.05670. $[\alpha]_D$: –44.6° (9.6 mg/ml, H_2O). HPLC purity = 97.9%; rt = 2.8 min (CH_3CN / H_2O 0:100 to 100:0 over 30 min).

*Plasmid and strain construction***.** For antibiotic susceptibility testing, the β-lactamase genes were cloned into the pTRC-99k vector, which is a derivative of pTRC99a (Pharmacia) obtained by replacing the β-lactamase resistance gene by a kanamycin resistance gene (Km, *lacI*, pTRC promoter, *ori*VcolEI; D. Mengin-Lecreulx, unpublished). Recombinant plasmids were introduced by electrotransformation into *E. coli* Top10. For β-lactamase production, fragments of the β-lactamase genes encoding soluble enzymes, *i.e.* devoid of the signal peptides, were cloned into the pET-TEV vector generating translational fusions with a vector-encoded N-terminal 6 x His tag followed by a TEV cleavage site (MHHHHHHENLYFQGHM).

Production and purification of β-lactamases. E. coli BL21 (DE3) harboring recombinant plasmids were grown in brain heart infusion (BHI) broth supplemented with kanamycin (50 µg/ml) at 37°C under vigorous shaking until the optical density at 600 nm (OD_{600}) reached 0.8. Isopropyl β-D-1-thiogalactopyranoside IPTG (0.5 mM) was added and incubation was continued at 16°C for 18 h. Bacteria were harvested by centrifugation, re-suspended in 25 mM Tris-HCl (pH 7.5) containing 300 mM NaCl (buffer A), and lysed by sonication. The enzymes were purified from clarified lysates by affinity chromatography (NiNTA agarose, Sigma-Aldrich) and size exclusion chromatography in buffer A (Superdex 200 HL26/60, Amersham Pharmacia Biotech). Protein concentration was determined by the Biorad protein assay using bovine serum albumin as a standard.

Determination of kinetic parameters. Kinetic parameters k_{cat}, K_m, and k_{cat}/K_m for hydrolysis of nitrocefin and CENTA were determined at 20 °C in 2-(*N*-morpholino)ethanesulfonic acid (MES; 100 mM; pH 6.4) by spectrophotometry, as previously described.[27] Briefly, the initial velocity (v_i) was determined by spectrophotometry for various concentrations of β-lactams [S] and a fixed concentration of β-lactamase [E]. The values of v_i were plotted as a function of [S]. The kinetic constants K_m and k_{cat} were determined by fitting the equation $v_i = k_{cat}$ [E] [S] / K_m + [S] to the resulting curve. The molecular extinction coefficient was 15,200 $M^{-1}cm^{-1}$ at 486 nm for nitrocefin and 7,380 $M^{-1}cm^{-1}$ at 415 nm for CENTA, respectively. Kinetic parameters for the carbamoylation of β-lactamases by DBOs (k_2/K_i and k_{-2}) were determined at 20°C in MES (100 mM; pH 6.4), as previously described.[7] The reporter substrate was nitrocefin (100 µM) for TEM-1, KPC-2, CTX-M-15, and $AmpC_{clo}$ or CENTA (100 µM) for OXA-48. Kinetics constants were deduced from a minimum of 6 progress curves obtained in a minimum of two independent experiments.

MIC determination. MICs of β-lactams were determined by the microdilution method in Mueller-Hinton (cation-adjusted) broth according to Clinical and Laboratory Standards Institute (CLSI) recommendations.[28] Diazabicyclooctanes were used at a fixed concentration of 15 µM (4 µg/ml for avibactam). Clavulanate was tested at 4 µg/ml. IPTG (500 µM) was added to the microdilution plates to induce production of the β-lactamase. The precultures were grown in BHI broth containing IPTG (500 µM) and kanamycin (50 µg/ml) for plasmid maintenance. Reported MICs are the medians from five biological repeats obtained in two independent experiments.

ASSOCIATED CONTENT

Supporting Information

The Supporting Information is available free of charge on the ACS Publications website.
Synthesis and characterization of alkyne **5f**, **5g** and **5i** (PDF)
Synthesis and characterization of relebactam (PDF)
NMR analysis (PDF)
Table of Kinetic constant k_{-2} (s^{-1}) for decarbamoylation of β-lactamases with synthesized compounds (PDF)

AUTHOR INFORMATION

Corresponding Author

*E.mail: laura.iannazzo@parisdescartes.fr; Phone: (33) 1 42 86 20 20;

*E.mail: melanie.etheve-quelquejeu@parisdescartes.fr; Phone: (33) 1 42 86 40 26;

*E.mail: michel.arthur@crc.jussieu.fr; Phone (33) 1 44 27 54 77.

Author Contributions

[I]These authors contributed equally.

Notes

The authors declare no competing financial interest.

ACKNOWLEDGMENT

This research was funded by grants from the Agence National de la Recherche (ANR), Project MycWall (N° ANR-17-CE18-0010-01). The authors are grateful to Atlanchim Pharma for the synthesis of compound **4** in large scale.

ABBREVIATIONS

CuAAC, copper-catalyzed alkyne-azide cycloaddition; DBO, diazabicyclooctane; DCM, dichloromethane; DMAP, *N*-dimethylaminopyridine; DMF, *N*-dimethylformamide; HPLC, high performance liquid chromatography; HRMS, high resolution mass spectroscopy; KPC, *Klebsiella pneumoniae* carbapenemases; MIC, minimal inhibitory concentration; NMR, nuclear magnetic resonance; TFA, trifluoroacetic acid; THF, tetrahydrofuran; TLC, thin layer chromatography.

REFERENCES

(1) Lobanovska, M.; Pilla, G., Penicillin's discovery and antibiotic resistance: lessons for the future? *Yale J. Biol. Med.* **2017**, *90*, 135-145.

(2) Zapun, A.; Contreras-Martel, C.; Vernet, T., Penicillin-binding proteins and beta-lactam resistance. *Fems Microbiol. Rev.* **2008**, *32*, 361-385.

(3) Bush, K.; Bradford, P., Interplay between β-lactamases and new β-lactamase inhibitors. *Nat. Rev.* **2019**, *17*, 295-306.

(4) Drawz, S. M.; Bonomo, R. A., Three decades of beta-lactamase inhibitors. *Clin. Microbiol. Rev.* **2010**, *23*, 160-201.

(5) Wang, D. Y.; Abboud, M. I.; Markoulides, M. S.; Brem, J.; Schofield, C. J., The road to avibactam: the first clinically useful non-beta-lactam working somewhat like a beta-lactam. *Future Med. Chem.* **2016**, *8*, 1063-1084.

(6) Ehmann, D. E.; Jahic, H.; Ross, P. L.; Gu, R. F.; Hu, J.; Durand-Reville, T. F.; Lahiri, S.; Thresher, J.; Livchak, S.; Gao, N.; Palmer, T.; Walkup, G. K.; Fisher, S. L., Kinetics of avibactam inhibition against Class A, C, and D beta-lactamases. *J. Biol. Chem.* **2013**, *288* , 27960-27971.

(7) Ehmann, D. E.; Jahic, H.; Ross, P. L.; Gu, R. F.; Hu, J.; Kern, G.; Walkup, G. K.; Fisher, S. L., Avibactam is a covalent, reversible, non-beta-lactam beta-lactamase inhibitor. *Proc. Natl. Acad. Sci. U. S. A.* **2012**, *109*, 11663-11668.

(8) Choi, H.; Paton, R. S.; Park, H.; Schofield, C. J., Investigations on recyclisation and hydrolysis in avibactam mediated serine beta-lactamase inhibition. *Org. Biomol. Chem.* **2016**, *14* , 4116-4128.

(9) Das, C.; Nair, N., Molecular insights into avibactam mediated class C β-lactamase inhibition: competition between reverse acylation and hydrolysis through desulfation. *Phys. Chem. Chem. Phys.* **2018**, *20*, 14482-14490.

(10) Krishnan, N. P.; Nguyen, N. Q.; Papp-Wallace, K. M.; Bonomo, R. A.; van den Akker, F., Inhibition of Klebsiella beta-Lactamases (SHV-1 and KPC-2) by Avibactam: A Structural Study. *PLoS One* **2015**, *10*, e0136813.

(11) Lizana, I.; Delgado, E. J., Molecular insights on the release of avibactam from the acyl-enzyme complex. *Biophys. J.* **2019**, *116*, 1650-1657.

(12) Levy, N.; Bruneau, J. M.; Le Rouzic, E.; Bonnard, D.; Le Strat, F.; Caravano, A.; Chevreuil, F.; Barbion, J.; Chasset, S.; Ledoussal, B.; Moreau, F.; Ruff, M., Structural basis for *E. coli* penicillin binding protein (PBP) 2 inhibition, a platform for drug design. *J. Med. Chem.* **2019**, *62*, 4742-4754.

(13) Papp-Wallace, K. M.; Nguyen, N. Q.; Jacobs, M. R.; Bethel, C. R.; Barnes, M. D.; Kumar, V.; Bajaksouzian, S.; Rudin, S. D.; Rather, P. N.; Bhavsar, S.; Ravikumar, T.; Deshpande, P. K.; Patil, V.; Yeole, R.; Bhagwat, S. S.; Patel, M. V.; van den Akker, F.; Bonomo, R. A., Strategic approaches to overcome resistance against Gram-negative pathogens using beta-Lactamase inhibitors and beta-lactam enhancers: activity of three novel diazabicyclooctanes WCK 5153, zidebactam (WCK 5107), and WCK 4234. *J. Med. Chem.* **2018**, *61*, 4067-4086.

(14) Xiong, H.; Chen, B.; Durand-Réville, T. F.; Joubran, C.; Alelyunas, Y. W.; Wu, D.; Huynh, H., Enantioselective Synthesis and Profiling of Two Novel Diazabicyclooctanone β-Lactamase Inhibitors. *ACS Med. Chem. Lett.* **2014**, *5* , 1143-1147.

(15) Durand-Réville, T. F.; Guler, S.; Comita-Prevoir, J.; Chen, B.; Bifulco, N.; Huynh, H.; Lahiri, S.; Shapiro, A. B.; McLeod, S. M.; Carter, N. M.; Moussa, S. H.; Velez-Vega, C.; Olivier, N. B.; McLaughlin, R.; Gao, N.; Thresher, J.; Palmer, T.; Andrews, B.; Giacobbe, R. A.; Newman, J. V.; Ehmann, D. E.; de Jonge, B.; O'Donnell, J.; Mueller, J. P.; Tommasi, R. A.; Miller, A. A., ETX2514 is a broad-spectrum β-lactamase inhibitor for the treatment of drug-resistant Gram-negative bacteria including Acinetobacter baumannii. *Nat. Microbiol.* **2017**, *2*, 17104.

(16) Ball, M.; Boyd, A.; Ensor, G. J.; Evans, M.; Golden, M.; Linke, S. R.; Milne, D.; Murphy, R.; Telford, A.; Kalyan, Y.; Lawton, G. R.; Racha, S.; Ronsheim, M.; Zhou, S. H., Development of a Manufacturing Route to Avibactam, a beta-Lactamase Inhibitor. *Org. Process. Res. Dev.* **2016**, *20*, 1799-1805.

(17) Blizzard, T. A.; Chen, H.; Kim, S.; Wu, J.; Bodner, R.; Gude, C.; Imbriglio, J.; Young, K.; Park, Y. W.; Ogawa, A.; Raghoobar, S.; Hairston, N.; Painter, R. E.; Wisniewski, D.; Scapin, G.; Fitzgerald, P.; Sharma, N.; Lu, J.; Ha, S.; Hermes, J.; Hammond, M. L., Discovery of MK-7655, a beta-lactamase inhibitor for combination with Primaxin (R). *Bioorg. Med. Chem. Lett.* **2014**, *24*, 780-785.

(18) Mangion, I. K.; Ruck, R. T.; Rivera, N.; Huffman, M. A.; Shevlin, M., A Concise Synthesis of a beta-Lactamase Inhibitor. *Org. Lett.* **2011**, *13*, 5480-5483.

(19) Miller, S. P.; Zhong, Y. L.; Liu, Z. J.; Simeone, M.; Yasuda, N.; Limanto, J.; Chen, Z.; Lynch, J.; Capodanno, V., Practical and Cost-Effective Manufacturing Route for the Synthesis of a beta-Lactamase Inhibitor. *Org. Lett.* **2014**, *16* , 174-177.

(20) Yang, S. W.; Xin, L. H.; Smith, E.; Pan, J. P.; Sprague, V.; Su, J., Synthesis of bicyclic beta-lactamase inhibitor relabactam derivatives from a relabactam intermediate. *Tetrahedron Lett.* **2017**, *58*, 2838-2841.

(21) Edoo, Z.; Iannazzo, L.; Compain, F.; Li de la Sierra Gallay, I.; van Tilbeurgh, H.; Fonvielle, M.; Bouchet, F.; Le Run, E.; Mainardi, J. L.; Arthur, M.; Etheve-Quelquejeu, M.;

Hugonnet, J. E., Synthesis of Avibactam Derivatives and Activity on beta-Lactamases and Peptidoglycan Biosynthesis Enzymes of Mycobacteria. *Chem.- Eur. J.* **2018**, *24*, 8081-8086.
(22) Kolb, H. C.; Finn, M. G.; Sharpless, K. B., Click chemistry: diverse chemical function from a few good reactions. *Angew. Chem. Int. Ed.* **2001**, *40*, 2004-2021.
(23) Ohnmacht, S.; Nava, P.; West, R.; Parker, R.; Atkinson, J., Inhibition of oxidative metabolism of tocopherols with omega-N-heterocyclic derivatives of vitamin E. *Bioorg. Med. Chem.* **2008**, *16*, 7631-7638.
(24) Bush, K.; Bradford, P. A., Interplay between beta-lactamases and new beta-lactamase inhibitors (vol 17, pg 295, 2019). *Nat. Rev. Microbiol.* **2019**, *17*, 459-460.
(25) Lahiri, S. D.; Mangani, S.; Durand-Reville, T.; Benvenuti, M.; De Luca, F.; Sanyal, G.; Docquier, J. D., Structural insight into potent broad-spectrum inhibition with reversible recyclization mechanism: avibactam in complex with CTX-M-15 and *Pseudomonas aeruginosa* AmpC beta-lactamases. *Antimicrob. Agents Chemother.* **2013**, *57*, 2496-2505.
(26) King, D. T.; King, A. M.; Lal, S. M.; Wright, G. D.; Strynadka, N. C. J., Molecular Mechanism of Avibactam-Mediated beta-Lactamase Inhibition. *Acs Infect. Dis.* **2015**, *1*, 175-184.
(27) Hugonnet, J. E.; Blanchard, J. S., Irreversible inhibition of the *Mycobacterium tuberculosis* beta-lactamase by clavulanate. *Biochemistry* **2007**, *46*, 11998-20004.
(28) Clinical and Laboratory Standards Institute, W., PA. , Methods for dilution susceptibility tests for bacteria that grow aerobically; approved standard. *Clin Lab Stand Inst M7–A8, 10th ed.* **2015**.

SYNOPSIS TOC (Word Style "SN_Synopsis_TOC"). If you are submitting your paper to a journal that requires a synopsis graphic and/or synopsis paragraph, see the Instructions for Authors on the journal's homepage for a description of what needs to be provided and for the size requirements of the artwork.